LAWRENCE
LIVERMORE
NATIONAL
LABORATORY

LLNL-JRNL-415058

PEAT ACCRETION HISTORIES DURING THE PAST 6000 YEARS IN MARSHES OF THE SACRAMENTO - SAN JOAQUIN DELTA, CALIFORNIA, USA

J. Z. Drexler, C. S. de Fontaine, T. A. Brown

July 27, 2009

Estuaries and Coasts

Disclaimer

PEAT ACCRETION HISTORIES DURING THE PAST 6000 YEARS IN MARSHES OF THE SACRAMENTO - SAN JOAQUIN DELTA, CALIFORNIA, USA

Judith Z. Drexler and Christian S. de Fontaine

U.S. Geological Survey California Water Science Center

6000 J Street, Placer Hall

Sacramento, California, USA 95819-6129

E-mail: jdrexler@usgs.gov, csdf@quaternary.org

and Thomas A. Brown

Center for Accelerator Mass Spectrometry

Lawrence Livermore National Laboratory L-397

PO BOX 808, 7000 East Avenue

Livermore, CA 94551

E-mail: tabrown@llnl.gov

ABSTRACT:

Peat cores were collected in 4 remnant marsh islands and 4 drained, farmed islands throughout the Sacramento - San Joaquin Delta of California in order to characterize the peat accretion history of this region. Radiocarbon age determination of marsh macrofossils at both marsh and farmed islands showed that marshes in the central and western Delta started forming between 6030 and 6790 cal yr BP. Age-depth models for three marshes were constructed using cubic smooth spline regression models. The resulting spline fit models were used to estimate peat accretion histories for the marshes. Estimated accretion rates range from 0.03 to 0.49 cm yr^{-1} for the marsh sites. The highest accretion rates are at Browns Island, a marsh at the confluence of the Sacramento and San Joaquin rivers. Porosity was examined in the peat core from Franks Wetland, one of the remnant marsh sites. Porosity was greater than 90% and changed little with depth indicating that autocompaction was not an important process in the peat column. The

mean contribution of organic matter to soil volume at the marsh sites ranges from 6.15 to 9.25% with little variability. In contrast, the mean contribution of inorganic matter to soil volume ranges from 1.40 to 8.45% with much greater variability, especially in sites situated in main channels. These results suggest that marshes in the Delta can be viewed as largely autochthonous vs. allochthonous in character. Autochthonous sites are largely removed from watershed processes, such as sediment deposition and scour, and are dominated by organic production. Allochthonous sites have greater fluctuations in accretion rates due to the variability of inorganic inputs from the watershed. A comparison of estimated vertical accretion rates with 20th century rates of global sea-level rise shows that currently marshes are maintaining their positions in the tidal frame, yet this offers little assurance of sustainability under scenarios of increased sea-level rise in the future.

KEY WORDS: autocompaction, marsh, porosity, radiocarbon age determination, sea-level rise, soil volume, vertical accretion

INTRODUCTION

Marshes form where hydrologic, geomorphic, and ecologic factors are conducive to the initial and continued accretion of mineral sediment and organic matter (Anisfield et al. 1999, Reed 2000). In freshwater tidal marshes, such accretion ultimately leads to the formation of peat soils. The rate at which peat vertically accretes varies both spatially and temporally. Spatial variability in accretion can be attributed to differences in ecological factors (e.g., plant community composition, plant productivity, and decomposition rates) and/or physical factors (e.g., tidal amplitude, duration of flooding, proximity to tidal creeks, and sediment load of channels) (Khan and Brush 1994, Hensel et al. 1998, Allen 2000, Merrill and Cornwell 2000, Reed 2002a, Temmerman et al. 2003, Schoellhamer et al. 2007, and Neubauer 2008). In contrast, temporal variation in accretion rates is largely caused by climatic fluctuations and extreme natural events such as fire and flooding that affect plant productivity and/or sediment supply in channels (Reed 2000, Allen 2000, Wright and Schoellhamer 2005, Schoellhamer et al. 2007). In addition, temporal and spatial changes in vertical accretion can be due to a wide range of human activities including land-clearing for agriculture, hydraulic mining for ore, and dam-building (Gilbert 1917, Orson et al. 1990, Wright and Schoellhamer 2005).

To date, most marsh studies incorporating temporal variability of accretion rates have focused on short time-scales of <10 yrs up to 100 yrs. These short-term accretion rates have been compared to current and predicted rates of future sea-level rise in order to assess the overall sustainability of coastal marshes (e.g., Stevenson et al. 1986, Penland and Ramsey 1990, Roman et al. 1997, Reed 2002a, Cahoon et al. 2006). Such studies clearly provide insights into the future behavior of marshes. However, due to their short time-scales, they cannot adequately portray the range of accretion rates that are feasible in particular marsh settings. For this reason, studies are also needed that estimate accretion processes over time-scales that approach or incorporate the entire lifetime of a marsh. Knowledge of long-term rates (millennial scale) can provide a broader context for understanding the intrinsic capability of marshes to continue providing crucial ecosystem services under scenarios of global climate change and associated sea-level rise.

Long-term accretion rates in peat are typically estimated using radiocarbon age determination over the entire depth of a peat deposit. Models are then used in order to interpolate between dated sections of the peat core. Research has shown, however, that the success of this approach relies heavily on avoiding methodological pitfalls and accounting for all possible error. For example, small depth intervals must be used between radiocarbon samples because larger intervals have been associated with dubious chronologies and highly varying accretion rates (Liu et al. 1992, Reed 2002a). Plant macrofossils must also be used for radiocarbon analysis and not bulk peat, because bulk peat consists largely of roots which are significantly younger than the actual surface of interest (Kaye and Barghoorn 1964, Tornqvist et al. 1992, van Heteren and van de Plassche 1997). Furthermore, all error related to choosing and analyzing a particular radiocarbon sample and using it to represent a particular depth interval needs to be incorporated into a model in order to provide realistic error estimates (Heegaard et al. 2005). In addition, peat cores need to be evaluated for the possibility of autocompaction, which involves settling of inorganic and organic fractions as well as loss of interstitial water in the saturated zone (Kaye and Barghoorn 1964). Approaches exist that can estimate autocompaction and these need to be explored if a significant relationship is found between depth and accretion rate (Kaye and Barghoorn 1964, Pizzuto and Schwendt 1997, Stevenson et al. 1986, Allen 2000). Lastly, for areas that are known to be tectonically active, an evaluation of the prospects of subsidence or uplift is essential for proper interpretation of the peat record (e.g., Atwater et al. 1977, Sawai et al. 2002, Tornqvist et al. 2004, Tornqvist et al. 2006).

The Sacramento-San Joaquin Delta (hereafter, the Delta) of California contains a long, continuous peat record, making it well-suited for studying peat accretion through the millennia. The Delta, which constitutes the landward limit of the San Francisco Bay Estuary, was once a 1400 km^2 tidal marsh that began forming ~6700 calibrated years before present (cal yr BP; Drexler et al. 2007). Between the 1860s and 1930s, the Delta was greatly transformed by drainage and extensive levee-building into an agricultural landscape with about 57 farmed islands and tracts (Thompson 1957, Ingebritsen et al. 2000). Such major changes in land use have resulted in land-surface subsidence of up to 8 m below sea level, due mainly to microbial oxidation of peat soils (Deverel and Rojstaczer 1996, Deverel et al. 1998, de Fontaine et al. 2009). The Delta ecosystem has also been strongly impacted by its use as a major water conveyance system for California via the State Water Project and the Federal Central Valley Project. Due to a number of factors including altered flows from massive pumps and management of salinity within a narrow range, several fish species are currently threatened or endangered (Service 2007). Currently, State and federal agencies are working to restore the general ecological health of the region. Wetland restoration has been one of the tools used to increase habitat for sensitive species and improve the general ecological health in the region (Reed 2002b). In addition, wetland restoration has the potential to mitigate land-surface subsidence by rebuilding peat (e.g., Miller et al. 1997) and, in so doing, provide the much-needed ecosystem service of sequestering carbon.

In order for wetland restoration to have the best chance of success, scientists and managers need information on peat accretion processes. Although there have been studies on peat distribution and peat thickness in the Delta (Atwater 1980, Atwater and Belnap 1980, Atwater 1982), little is currently known about how peat started forming and how quickly it has accreted through time. In a rare paper on the Quaternary evolution of the Delta, Shlemon and Begg (1975) determined 10 radiocarbon dates at progressively deeper depths along an east-west transect in the Delta. Due to the use of large sampling intervals and bulk peat, the data cannot be used to estimate vertical accretion rates. Nevertheless, these data provide an important baseline of peat age against which to compare subsequent data. Methodological issues also exist for a paper by Atwater et al. (1977), which contains a valuable data set of radiocarbon analyses from salt marshes in south San Francisco Bay, the most seaward part of the San Francisco Bay Estuary. More recently, Goman and Wells (2000) determined vertical accretion rates for two peat cores collected at Browns Island, one of the sites chosen for this study. They used linear models and found high variability in accretion with depth (0.05 - 0.41 cm yr^{-1}). Reed (2002) is the only study to focus on recent accretion rates in the Delta. Over a two-year period, Reed (2002b) determined that rates of vertical accretion were in excess of 1 cm yr^{-1} in restored and references marshes, with highest rates at sites closest to the Sacramento River and lowest rates in interior marsh sites.

Clearly, more information is needed on the variability and characteristics of peat accretion in the Delta through time. This information is of particular importance to managers and scientists responsible for maintaining the elevation of historic and restored marshes with respect to the tidal frame. For these reasons, we made a comprehensive study of peat accretion rates in four relatively undisturbed marshes in the Delta. Four additional farmed islands were studied to understand initial peat formation processes. The chief goals of the study were to answer the following questions: (1) how might peat have initially started forming in the Delta, (2) how quickly has peat accreted through the millennia? and (3) given past performance, are the remnant Delta marsh islands capable of keeping pace with current and future rates of sea-level rise?

STUDY SITES

The Delta is located at the confluence of the Sacramento and San Joaquin Rivers and receives runoff from over 40% of the land area of California (California Department of Water Resources 1995) (Figure 1). During the last few hundred years, the Delta has been exclusively a freshwater tidal system, however current geochemical research suggests that salinity may have been brackish during at least some of its history (Charles Alpers, U.S. Geological Survey, unpublished data). Tides are semidiurnal with normal tidal range of approximately one meter, however, during floods river stage can exceed two meters (Shlemon and Begg 1975, Atwater 1980). The climate in the Delta is characterized as Mediterranean with cool winters and warm, dry summers (Atwater 1980). Mean annual precipitation is approximately 36 cm, but actual yearly precipitation varies from half to almost four times this amount. Over 80% of precipitation occurs from November through March (Thompson 1957). Beginning in the mid-1800s, the Delta was largely drained for agriculture (Thompson 1957, Atwater 1980), resulting in its current configuration of over

100 islands and tracts surrounded by 2250 km of man-made levees and 1130 km of waterways (Prokopovich 1985). Subsequent to drainage, the farmed islands experienced land-surface subsidence. Recent rates of land-surface subsidence range from approximately 0.5–3.0 cm yr^{-1}(Rojstaczer and Deverel 1993, 1995, Deverel and Leighton, 2008). Land-surface subsidence due to natural gas extraction and groundwater withdrawal is estimated to be approximately 0.508 cm yr^{-1} in the north and northeastern parts of the Delta, but this gas field is largely outside the area covered by this study (Rojstaczer et al. 1991). Current rates of subsidence due to gas extraction and groundwater withdrawal are unknown. Neotectonic subsidence and uplift of ~0.2 to 0.6 mm yr^{-1} are thought to be occurring along the west and east side, respectively, of the Midland Fault, which runs approximately north to south bisecting the Delta at Sherman Island (Weber-Band 1998).

Study sites were chosen to encompass the various geomorphic settings and salinity regimes of the Delta. Sites were chosen along the historic floodplain of the Sacramento River as well as the glacial outwash area along the San Joaquin River. In addition, sites were selected from high energy environments such as the confluence of the Sacramento and San Joaquin Rivers to more quiescent environments such as distributaries of the San Joaquin River. In total, eight sites were chosen including four remnant, relatively undisturbed marsh islands and four nearby drained farmed islands (Figure 1). Cropping histories for the farmed islands are available in de Fontaine et al. (2009). On each of the farmed islands, coring was done both near the levee and near the center of the island because land-surface subsidence is known to be significantly greater at the center of the islands (Ingebritsen and Ikehara 1999, Mount and Twiss 2005). Coring on the marsh islands was only done near the island centers. Table 1 contains site abbreviations, locations, elevations, sizes, and periods of drainage and levee building.

The remnant marsh islands are much smaller than the farmed islands, and because of that, they were not drained for agriculture. Vegetation on the marsh islands is dominated by emergent macrophytes and shrub-scrub wetland species. On Browns Island (BRI), the most brackish of the study sites, vegetation is dominated by *Schoenoplectus americanus* (American bulrush) and *Distichlis spicata* (salt grass). On the channel island northwest of Bacon Island (BACHI) the overstory is dominated by *Salix lasiolepis* (arroyo willow) and the understory is dominated by *Cornus sericea* (red-osier dogwood) with smaller amounts of *Phragmites australis* (common reed) and *Rosa californica* (California wild rose). On Franks Wetland (FW) the vegetation is dominated by *Cornus sericea* and *Salix lasiolepis*, with the coring site having a large population of *Athyrium filix-femina* (western lady fern). The tip of Mandeville Tip (TT) is dominated by *Cornus sericea* and *Salix lasiolepis*. Several species such as *Schoenoplectus acutus* (hardstem bulrush), *Phragmites australis*, and *Typha* spp. are found at all sites. All botanical nomenclature follows Hickman (1993).

METHODS

Field Work

In the summer of 2005, peat cores from the marsh islands and farmed islands were retrieved using a modified 5-cm-diameter Livingstone corer (Wright 1991). Cores were

collected in multiple drives all the way to refusal in the underlying mineral sediment to ensure that the entire peat column was retrieved. Total peat thicknesses are shown in Table 2. Core drives were extruded onto cellophane-lined PVC tubes cut longitudinally in half, photographed, and visually described regarding color and texture in the field. The cores were quickly wrapped in cellophane, covered with the other longitudinal half of the PVC tube, and taped shut. All cores were immediately placed in a large cooler until being transported to the laboratory where they were stored in a refrigerator at approximately 3°C. At BRI, a soil monolith containing the top 49 cm was dug out because the root mat was too dense to collect with the Livingstone corer. Below the monolith, a peat core of 775 cm in depth was collected (BRIC4). After analysis, it was discovered that this depth was not sufficient to reach the underlying mineral substrate, even though much clay was already present below 700 cm. Therefore, an additional core, with peat thickness of 922 cm, was collected in March of 2007 within 2 m of the original coring site.

Real-time kinematic (RTK) geographic positioning was used to establish the elevations and coordinates of the coring locations. Full details of the RTK survey can be found in de Fontaine et al. (2009). Ellipsoid heights from the RTK survey were converted to orthometric elevations (NAVD88) using a GEOID03 model. Tidal benchmark LSS 13 (NOAA tidal station 9415064 on the San Joaquin River near Antioch, CA) with a static surveyed ellipsoid height of -28.75 m was used to adjust the elevations of the coring sites to local mean sea level (MSL). Based on the height difference of 14 overlapping survey points from different base stations, the error of the core-site elevations is estimated to be ±0.075 m.

Laboratory Work

In the laboratory, cores were individually unwrapped, split lengthwise and immediately photographed. Core stratigraphy was documented, and one longitudinal half of the core was wrapped in cellophane and archived for future use. Bulk density was obtained by sectioning cores into 2-cm-thick blocks, measuring each dimension, obtaining wet weight of the sample, drying overnight at 105 °C, and then weighing again to obtain dry weight (Givelet et al. 2004). Core data were examined for compression and/or expansion, but no mathematical corrections were needed. The only correction made was to remove a small amount of peat from the top and bottom of some drives (generally < 4 cm) when it was visually apparent that the drives contained non-contiguous peat from elsewhere in the core. The presence of non-contiguous peat was confirmed in the laboratory by anomalous bulk density values that differed from the rest of the drive. The peat monolith from BRI expanded upon removal from the marsh surface. The amount of expansion was determined and the core data were corrected accordingly. Basal contacts of the peat columns with the underlying epiclastic sediment were generally sharp and could usually be determined by a spike in bulk density for sections immediately beneath the peat. At one site (BRI), however, the transition from peat to epiclastic sediment is gradual. Therefore, we also used the definition of an organic soil to differentiate peat from underlying mineral sediments. Saturated organic soils by definition must have an organic carbon content (by weight) of (1) > 18% if the mineral fraction has 60% or more clay, (2) > 12% if the mineral fraction contains no clay, or (3) > 12% + (clay percentage multiplied by 0.1 %) if the

mineral fraction contains less than 60% clay (United States Department of Agriculture Soil Conservation Service 2006).

Organic fragments for radiocarbon analysis were sampled directly from the split core face where visible, or a 2- to 4-cm-thick sample of peat was sieved to concentrate seeds, charcoal or other terrestrial macrofossils. *Schoenoplectus* achenes in particular were sought out as these were well distributed in the peat cores and have been shown to be a reliable material for radiocarbon dating of peat layers (Wells 1995). Radiocarbon samples were analyzed by Accelerator Mass Spectrometry (AMS) at the Center for Accelerator Mass Spectrometry (CAMS), Lawrence Livermore National Laboratory (LLNL) in Livermore, California. Ages were calibrated using CALIB (version 5.0.1 (Stuiver and Reimer 1993) with the INTCAL04 curve (Reimer et al. 2004)). All details related to the radiocarbon data used in this study are shown in Appendix 1.

Test for Autocompaction

In order to test for autocompaction, we focused on the change in porosity with depth in the peat column. Previous research has indicated that peats with porosities greater than 75% are "poorly compacted" (Kaye and Barghoorn 1964). We calculated particle densities of peat (ρ_o) using the empirical equation from Okruszko (1971), who studied nearly 3000 peat samples with ash contents ranging from 0.7 – 99.5%:

$$\rho_o = 0.011 * (IM) + 1.451 \text{ (g cm}^{-3}\text{)} \quad \text{(I)}$$

where IM = % ash content. The following equation from Hillel (1998) was used to calculate porosity Φ (%):

$$\Phi = 1 - (BD/\rho_o) \quad \text{(II)}$$

Inorganic vs. Organic Contribution to Soil Volume

The relative contributions of organic matter vs. inorganic matter to soil volume (OM_v and IM_v, respectively) were calculated as follows:

$$\% OM_v = BD*LOI/1.1 \quad \text{(III)}$$

$$\% IM_v = (BD*(100-LOI))/2.6 \quad \text{(IV)}$$

where BD = bulk density (g cm^{-3}) of marsh peat at a particular depth, LOI (loss on ignition in %), 1.1 g cm^{-3} is the particle density of organic matter, and 2.6 g cm^{-3} is the particle density of inorganic sediment (DeLaune et al. 1983).

Statistical Analysis

Cubic smooth spline regression models (hereafter, spline fit models) for BRI, FW, and BACHI were constructed following the statistical approach of Heegaard et al. (2005), who used a mixed effect regression model in order to incorporate (1) an error estimate for each individual object (within object variability of dated macrofossils) and (2) an error estimate for how representative each dated object is in relation to the sampled layer (between object variability). This approach also includes a loess smoothing procedure which combines linear least squares regression with nonlinear polynomial regression by fitting simple models to localized subsets of the data. For each marsh data set, diagnostic plots (residuals vs. fitted, square root of absolute residuals vs. fitted, observed versus fitted, and a qq-normplot) were examined to assess normal distribution of data and residuals. These plots together with variance plots were also examined in order to determine whether a constant variance or a μ variance was a better choice for the data. The median of the calibrated age distributions for the various macrofossils were used in the age-depth models, but where multiple dates were available for a particular depth, *Schoenoplectus* achenes were preferentially chosen due to their proven dependability in dating peat layers (Wells 1995). Radiocarbon dates for which the "between object" variability was large in comparison to the "within object" variability were identified as possible outliers (Heegaard et al. 2005). Outliers, which indicate an inversion in the stratigraphy or a discontinuity with depth, were closely examined and only removed from the data set when they were notably different from any other nearby data points. Several iterations of each age-depth model were carried out in order to determine what level of smoothing was needed to best represent the overall shape of the curve. The resulting age-depth models were constructed with 95% confidence envelopes. It is important to note that, with this approach, the greater the radiocarbon data set (n), the greater the confidence in the resulting spline fit model (Heegaard et al. 2005).

RESULTS

The radiocarbon data, when plotted by depth from the peat surface, form two main groups, which are largely linearly distributed (Figure 2a). The first group consists of the marsh sites and is found on the right side of Figure 2a. The second group consists of the farmed sites and is situated on the upper left of Figure 2a. The top part of the peat column from the farmed islands has been lost due to land-surface subsidence, making the peat column much thinner and older than at the marsh sites. Radiocarbon data from Shlemon and Begg (1975), shown in Figure 2a, straddle the data from this study. More of their data points occur to the right of the main line, indicating slightly younger ages of the bulk peat samples used in their study. Below 1000 cm the dates reported by Shlemon and Begg (1975), which are for Sherman Island at depths of 1220 cm and 1520 cm, seem improbably deep for peat (see definition for organic soil in Laboratory Methods), but highly possible for organic silts and clays found below the peat column. The oldest peats in this study are found in Webb Tract Levee (WTL), Webb Tract Center Island (WTCI), and Venice Island Prisoner's Point (VIPP) and date to approximately 6700 yr BP (Figure 2, Table 2). In Figure 2b, all the radiocarbon data are plotted relative to mean sea level. Figure 2b also includes radiocarbon data from Atwater et al. (1977) for plant roots, plant fragments, and other organic materials from south San Francisco Bay.

Spline fit models were constructed for the marsh sites BACHI, FW, and BRI, and a polynomial trend line was determined for TT, which had too few data points for a spline fit (Figure 3). Spline fit models were not constructed for the farmed islands because most of the peat column has been lost due to subsidence and the remaining peat is highly compacted, precluding its use in estimating accretion rates. Diagnostic and variance plots indicated that constant variance was the best fit for each of the 3 cubic smooth spline regressions. For each of the resulting spline fit models, the estimated ages are shown up until 250 yr BP or the most modern sample date available. More recent radiocarbon samples were not analyzed as such ages are difficult to interpret conclusively unless intensive techniques such as wiggle-matching of closely spaced samples are employed (Turetsky et al. 2004). For FW, the spline fit model fluctuates slightly in slope within the top 5.8 m MSL of the peat record. Below 5.8 m in elevation there were major age reversals in the stratigraphy from FW, and therefore, these data were omitted from the age-depth model. The model for BRI, on the other hand, has a less linear pattern, with major increases in slope between -4.0 to -6.0 m and -8.5 to -9.0 m in depth relative to MSL. The transition from Core 4 to Core 5 shows some divergent points that fall outside the 95% confidence interval, especially at -5.61 and -6.25 m, however this variability falls largely outside the two increases in slope. The age-depth model for BACHI also departs from linearity. There are two depth ranges, between approximately -1.5 to -2.0 m and -4.0 to -4.5 m relative to MSL, where sharp increases in slope are found.

The core from FW was chosen to check for autocompaction via changes in porosity because it has highly consistent measurements of bulk density and % OM along much of its depth and a high organic content through the core (Drexler et al. 2009). A high mean organic content indicates that the core is theoretically highly compressible (Kaye and Barghoorn 1964). Overall, the average porosity for FW between 0.8 – 5.8 m below MSL decreases slightly from approximately 96% to 94% (data within oval, Figure 4). Such high porosity values decreasing only slightly with depth indicate that autocompaction is probably minimal. The zones of higher porosity near the marsh surface are due to increased inorganic sediments and the higher porosities below -5.8 m reflect the increase in epiclastic sediments near the bottom of the peat column (Drexler et al. 2009). Such an apparent lack of autocompaction in the FW core suggests that the other marsh cores, which have similar or less organic content, are also largely free from autocompaction. However, we cannot be sure there is no autocompaction in Delta peat because we have no data on other aspects of autocompaction such as the collapse of plant fibers and decomposition effects (Kaye and Barghoorn 1964, Allen 2000). Therefore, vertical accretion rates reported here will be considered conservative estimates.

Yearly accretion estimates were calculated based on the spline fit functions shown in Figure 3 for FW, BACHI, and BRI (Figure 5, Table 3). For TT, accretion was calculated linearly between 100 - 1210 cal yr BP (0.13 cm yr^{-1}) and between 2340 - 1210 cal yr BP (0.21 cm yr^{-1}). FW has the least variable and lowest estimated mean accretion rate (0.12 cm yr^{-1}, sd = 0.03), while BRI has the most variable and highest estimated mean accretion rate (0.19 cm yr^{-1}, sd = 0.12). For FW, there are gently alternating periods of higher and lower estimated accretion rates that range between 0.03 – 0.16 cm yr^{-1}. BRI has two periods of high estimated accretion rates: (1) near the core bottom, and (2) between -4.0

and -5.5 m relative to MSL. BACHI also has variable estimated accretion rates (0.07 – 0.38 cm yr-1, Table 3), with two major peaks at approximately -1.7 and -4.1 m MSL.

The marsh peats form two basic groups, FW and BACHI vs. BRI and TT, based on their physical characteristics. In the first group mean % organic matter is greater than 70% and mean bulk density is less than < 0.15 g cm^{-3} (Table 4). With respect to the organic and inorganic contributions to soil volume (OM_v and IM_v, respectively) mean OM_v contributes about 2.5 times more than IM_v to soil volume at FW and mean OM_v contributes almost 5 times more than IM_v to soil volume at BACHI (Table 5). In contrast, mean % organic matter at BRI and TT is approximately 40% and mean bulk density is 0.31 and 0.23 g cm^{-3}, respectively (Table 4). The mean contributions of OM_v to IM_v are similar for both BRI and TT (Table 5). Below approximately 1 m relative to MSL in both the BACHI and FW cores, IM_v is less than ~2% until the bottom of the peat column (Figure 6). In contrast, at BRI and TT, IM_v is much more variable with depth in the peat column (Figure 6). IM_v reaches over 20% at mid-core at BRI as well as near the contact with epiclastic sediments for both BRI and TT. Both IM_v and OM_v increase toward the marsh surface at all marsh sites (Figure 6).

DISCUSSION

Peat formation and subsidence

The basal peats found in this study date to between 6030 – 6790 cal years BP (Table 2). These results suggest that peat started forming in the central and western Delta at largely the same time when sea-level rose and finally inundated the large, flat pre-Holocene valley at the landward end of the San Francisco Estuary (Figure 2, Table 2). In their 1975 paper, Shlemon and Begg came to another conclusion; namely, that peat initially formed on the western edge of the current Delta and spread easterly across the rest of the region. They came to this conclusion, however, based on the evidence of 10 radiocarbon dates spread across the Delta and one basal peat date from Sherman Island only. Their basal peat date from Sherman Island is older (median age of 7668 cal yr BP) than what was found in this study. This older date is certainly possible, because older and deeper pockets of peat may underlie the continuous layer of peat in the current Delta. In addition, it is also possible that this date refers not to peat *per se* but instead to organic material incorporated in organic muds or lacustrine sediments found beneath the peat column (personal communication, Roy Shlemon). This basal date for Sherman Island is coexistent with some marsh deposits from San Francisco Bay (Atwater et al. 1977, Figure 2b). Marshes in San Francisco Bay, however, most likely formed before Delta marshes due to the lower elevation of the Bay relative to the Delta and the proximity of the Bay to the Pacific Ocean. Therefore, considering the data available, it appears that peat deposits in the Delta started forming approximately 6800 years ago, which is consistent with the stabilization of sea-level about 6000 - 8000 years ago when many other deltas and associated wetlands started forming around the world (Stanley and Warne 1994).

Peat profiles of the radiocarbon data provide an unusual perspective regarding the legacy of draining marshes for agriculture (Figure 2a). In Figure 2, peat ages from the

farmed islands fall into an entirely different group from the marsh islands because the top 3000+ years worth of accretion (approximately 2/3 of the peat column) have been lost due to land-surface subsidence (Figure 2; Drexler et al. 2009). Much of the remaining peat on the farmed islands has also been shown to be compacted (Drexler et al. 2009). For these reasons, radiocarbon dates from the farmed islands could not be used to construct age-depth models or estimate vertical accretion rates.

Vertical accretion

Rates of vertical accretion per year were estimated from the spline fit functions for FW, BRI, and BACHI (Figures 3 and 5). It is important to note that the greater the number of radiocarbon dates for each site (n), the less the uncertainty of the resulting spline fit models (Heegaard et al. 2005) and, hence, the better the estimates of accretion. Therefore, BRI (n=27) has the best estimates relative to FW (n=9) and BACHI (n=12). Despite any limitations due to sample size, however, the construction of spline fit age-depth models and the estimation of yearly accretion rates are clearly an improvement over using simple linear models to produce a few sporadic estimates of accretion. Such a method of estimating accretion rates permits a rare view into the entire accretion history of these marshes. Estimated rates of peat accretion of the marsh sites ranged between 0.03 and 0.53 cm yr^{-1} (Figure 4, Table 3). Estimated mean accretion rates at BRI, BACHI, and FW were 0.19 (sd = 0.12), 0.16 (sd=0.09), and 0.12 cm yr^{-1} (sd=0.03). The accretion history for TT could not be estimated because there were not enough radiocarbon data to construct a spline fit model for this site. Because some peat undoubtedly has been lost through decomposition, vegetation compaction, and loss of porosity through time (however minor, see Figure 4), these estimates for vertical accretion are likely conservative estimates. Compared to recent rates of land-surface subsidence on farmed islands in the Delta (0.5–3.0 cm yr^{-1}; Rojstaczer and Deverel 1993, 1995, Deverel and Leighton, 2008), estimated rates of vertical accretion are quite low. However, in comparison to other peatlands, estimated vertical accretion rates for the Delta are greater than some millennial rates in inland boreal regions (e.g., 0.05 cm yr^{-1} over 6000 yr from Zoltai and Johnson 1985; 0.04 – 0.06 cm yr^{-1} over 1200 yr from Robinson and Moore 1999), within millennial rates in salt marshes in the northeastern United States (e.g., 0.11 – 0.25 cm yr^{-1} over the past 4000-5000 yr; Bloom 1964, Redfield 1967, Bartberger 1976, Keene 1971), and similar to previously published rates for BRI (0.05 - 0.41 cm yr^{-1} over ~6000 yr, Goman and Wells 2000).

There are important differences between the marsh sites regarding vertical accretion estimates and peat characteristics. Overall, the mean estimated rate of accretion and the range of yearly accretion estimates for FW are lower than the other sites. In addition to having higher mean rates of vertical accretion, BACHI and BRI have increasingly variable patterns through time (Table 3, Figure 5). With respect to peat characteristics, FW and BACHI both have mean organic matter content over 70% (Table 4) and bulk density below 0.15 g cm^{-3} (Table 4). In addition, for both cores, IM_v is very low through most of the peat profile (Table 5, Figure 6). These characteristics suggest that FW is a highly organic marsh site largely removed from watershed processes (i.e., sediment deposition and/or scour) and, therefore, is predominantly autochthonous with respect to peat formation. A

comparison of accretion rates vs. IM_v and OM_v contributions with depth at FW shows that there are corresponding increases in both IM_v and OM_v at the major accretion peaks in the core (i.e., at depths ~-1.1m, -3.7m, and -5.3 m MSL). However, such changes are quite subtle. BACHI, with its variable accretion rate appears to have characteristics of both an autochthonous and allochthonous site, however, due to its low IM_v, it tends more toward being autochthonous. A large increase in OM_v between approximately -1.0 and -2.25 m MSL suggests that authochthonous production at BACHI is of particular importance in this interval (Figure 6). BRI and TT, on the other hand, have much lower mean organic matter content than the other marsh sites (~40%; Table 4), greater mean bulk density (0.31 and 0.23 g cm^{-3}, respectively; Table 4), and considerable variability of IM_v throughout the peat profile (Figure 6). This suggests that BRI and TT are more responsive to watershed processes than FW and BACHI. BRI and TT appear to alternate between periods of being allochthonous and periods of being autochthonous. In the case of BRI for which there is a spline fit model, this shift between allochthonous and autochthonous behavior corresponds directly to periods of higher and lower peat accretion (Figures 5 and 6). Overall, IM_v is much more variable than OM_v in all of the marsh cores suggesting that much of the variability in peat accretion through time is related to changing allochthonous inputs.

The variability in allochthonous inputs most likely stems from climatic changes through time. The Delta region has considerable variability in precipitation rates and, thus, river flows (Thompson 1957). This translates into variability in the amount of suspended sediment transported into the rivers and available for peat formation. Peat accretion rates at BRI and BACHI appear to reflect dramatic increases and decreases in sediment supply over time. One period of especially high accretion rates, between approximately 4400 and 3100 cal yr BP (Figure 5), has been shown to be a very wet period in California history. During this time, the elevation of the treeline in the White Mountains of eastern California was higher than during the period from 2000 yr BP to present, when climate became dryer (LaMarche 1973). Research from Mono Lake shows the beginning of a unusual high stand of the lake starting at approximately 3800 cal yr BP (Stine 1990). Even the Mojave Desert of California was especially wet during this time. Enzel et al. (1989) document the presence of an ephemeral lake that formed in the Mojave approximately 3600 yr BP (Enzel et al. 1989).

In salt marsh research, authochthonous marshes are usually found in micro-tidal settings, while allochthonous marshes are found in settings with larger tidal range (French 2006, Allen 2000). This characterization needs to be revised for tidal freshwater marshes in the Delta because although tidal range in the Delta can be classified as microtidal (< 2 m), a slight decrease in tidal range across the Delta does not appear to have any influence over peat accretion processes. What does appear to influence peat accretion and contributions of IM_v and OM_v in the Delta is the proximity of marshes to flows in the main channels, a factor shown to be directly related to accretion rates in salt and freshwater tidal marshes (e.g., Hatton et al. 1983, Merrill and Cornwell 2000). In the Delta, however, marshes situated in highly exposed, high energy settings (i.e., BRI and TT, Table 1) have the highest accretion rates and IM_v *as well as* the highest variability in these values through time. These sites are most apt to be affected by major changes in river discharge and hence sediment deposition.

At all the marsh sites, there is an increase in both OM_v and IM_v to soil volume near the peat surface (Figure 6). This may be due to the lack of consolidation of organic matter at the surface in comparison to deeper in the peat column. With respect to the inorganic contribution to soil volume, the increase right near the surface could reflect the huge plug of suspended sediment carried into the Delta during hydraulic mining activities in the late 1800s and early 1900s (Gilbert 1917, Orr et al. 2003).

Future marsh sustainability

Marsh sustainability is determined by the ultimate balance between marsh vertical accretion and relative sea-level rise, which includes eustatic sea-level rise and any subsidence or uplift of the land surface. An indication of the capability of a marsh to maintain its position within the tidal frame can be found by comparing mean accretion rates for marshes in this study with current and future rates of sea-level rise. The estimated mean accretion rate of each marsh is well within the 0.1 – 0.2 cm yr^{-1} estimated rate of relative sea-level rise during the past 6000 years in the San Francisco Bay Estuary (Atwater et al. 1977) and very close to the estimated 20^{th} century rate of sea-level rise of 0.17 cm yr^{-1} (sd = 0.03) (Church and White 2006) (Figure 4, Table 3). FW is the only site for which the mean accretion rate and the upper bound of its estimated accretion range are below the 0.17 cm yr^{-1} value. However, considering the uncertainties involved in both the accretion estimates for FW and the Church and White (2006) sea-level rise estimate, FW is still within the error margin for keeping pace with sea-level rise. The current global rate of sea-level rise can be regionally adjusted by the estimated neotectonic displacement along the Midland Fault which amounts to approximately 0.4 mm yr^{-1} (midpoint value of 0.2 to 0.6 mm yr^{-1} range) of uplift on the west side of the Midland Fault (for BRI) and the same level of subsidence on the eastern side of the fault at BACHI and FW (Weber-Band 1998). Upon incorporating such displacement, the relative sea level rise becomes greater than mean vertical accretion at both FW and BACHI but not for BRI, which benefits from uplift. Under this scenario, only BRI could keep pace with current sea level rise. It is unclear, however, whether incorporating this estimate for neotectonic displacement is useful in determining how these marshes will fare with respect to sea level rise as neotectonic activity may average approximately 0.4 mm yr^{-1} over a long time span, but actual yearly movement is likely to be quite variable through time as well as space (Sawai et al. 2001, Shennan et al. 1998, Witter et al. 2003). Regarding the future, all of the estimated mean accretion rates are considerably less than the 0.38 cm yr^{-1} estimate for sea-level rise forecast for 2090-2099 (Intergovernmental Panel on Climate Change (IPCC) central estimate (scenario A1B) among six scenarios, which range from 0.15 – 0.97 cm yr^{-1}; Meehl et al. 2007). This predicted central estimate, however, is still within the total range of estimated accretion rates for both BACHI and BRI (Table 3).

It is important to note that even if Delta marshes are intrinsically capable of keeping pace with sea-level rise, the current availability of sediment may not be enough to keep marshes from being inundated. In the Delta as well as elsewhere, major dam construction has resulted in dramatic decreases in channel sediment loads (Yang et al. 2003, Schoellhamer et al. 2007). In the Sacramento River alone, suspended sediment

concentrations have decreased approximately 50% since major dam-building occurred in the 1960s (Wright and Schoellhamer 2004). Currently, it is unknown what effect this reduction in sediment availability has had on peat accretion rates in the Delta. The results from this study indicate, however, that Delta marshes depend on inputs of inorganic sediment, especially those situated in the main channels. Quantification of the recent relationships among reduced sediment loads, sedimentation rates, and peat accretion rates is therefore needed to better predict how marshes will fare in the future.

ACKNOWLEDGMENTS

This study was funded by the CALFED Science Program of the State of California Resources Agency, Agreement #F-O3-RE-029. We thank Jim Orlando, Jacob Fleck, Matt Kerlin, Curt Battenfeld, Stephanie Wong, Patricia Orlando, and Nicole Lunning for their help in the field and/or lab. Greg Pasternack of the University of California, Davis generously provided laboratory facilities for much of the analyses. Michelle Sneed, Gerald Bawden and Marti Ikehara provided critical guidance with the elevation survey. We also thank Anna Frampton for Polish translation and Neil Willits (Department of Statistics, UC Davis) for statistical advice. This work performed under the auspices of the U.S. Department of Energy by Lawrence Livermore National Laboratory under Contract DE-AC52-07NA27344.

Table 1. Basic descriptions of coring sites in the Delta. Salinity data represent typical, non-drought conditions in adjacent sloughs and are based on Atwater (1980). Mixohaline (brackish) refers to a range of approximately 0-10 ppt, with higher salinities found during the dry season. Terminology follows Mitsch and Gosselink (2000). Descriptions of hydrogeomorphic settings follow those described in Atwater (1980). SR is Sacramento River, SJR is San Joaquin River, NA is not applicable.

Coring Site Name	Island size (ha)	Elevation (MSL in m)	Salinity Regime in Channel	Hydrogeomorphic Setting	Relative Energy Regime	Period of Drainage and Levee Building
Browns Island (BRI)	268	0.51	Mixohaline	Confluence of SR and SJR	High	NA
Sherman Island, Levee (SHERL)	4205	-4.44	Mixohaline	Confluence of SR and SJR	High	1870–1880
Sherman Island, Center Island (SHERCI)	4205	-4.52	Mixohaline	Confluence of SR and SJR	High	1870–1880
Franks Wetland (FW)	28	0.27	Fresh	Distributary of SJR, sheltered by natural marsh breakwaters, adjacent to permanently flooded farmed island	Very Low	NA
Webb Tract, Levee (WTL)	2205	-5.18	Fresh	Main channel SJR and within historic floodplain of SR	Medium	1910–1920
Webb Tract, Center Island (WTCI)	2205	-7.25	Fresh	Main channel SJR within historic floodplain of SR	Medium to low	1910–1920
Mandeville Tip, Tip of Tip (TT)	12	0.20	Fresh	Glacial outwash region in main channel of SJR	Medium	NA
Venice Island Prisoners' Point, Levee (VIPP)	1263	-4.52	Fresh	Glacial outwash region in main channel of SJR	Medium	1900–1910
Venice Island, Center Island (VICI)	1263	-6.95	Fresh	Glacial outwash region in main channel of SJR	Medium to low	1900–1910
Bacon Island, Channel Island (BACHI)	10	0.21	Fresh	Glacial outwash region along distributary of SJR	Low	NA
Bacon Island, Levee (BACL)	2257	-5.86	Fresh	Glacial outwash region along distributary of SJR	Low	1910–1920
Bacon Island, “Point C” (BACPTC)	2257	-6.28	Fresh	Glacial outwash region along distributary of SJR	Low	1910–1920

Table 2. Ages of basal peat from each of the coring sites. Duplicate dates are available for some sites where radiocarbon analyses were done on multiple macrofossil types for the same depth interval. CAMS is the Center for Accelerator Mass Spectrometry at Lawrence Livermore National Laboratory. Calibrated ages are the median of the 2σ probability distribution (2σ ranges in parentheses) calculated by CALIB (Stuiver and Reimer, 1993, v5.0.1). [$]The macrofossil is from 912 cm, while the peat column extends to 922 cm. **These coring sites were on drained farmed islands subject to compaction and major land-surface subsidence. [#]Signifies the deepest date in the peat column before a series of age reversals extending to 718 cm in depth.

Coring Site	Peat thickness (cm)	Depth relative to MSL (cm)	CAMS Lab Code	Radiocarbon Age (^{14}C yr BP)	Calibrated Age (cal yr BP)	Macrofossil Type
BRI[$]	912	-861	133146	5600 ± 70	6233 (6031-6293)	Achenes
SHERL**	317	-761	126714	5670 ± 35	6450 (6325–6550)	Achenes
SHERL**	317	-761	126724	5740 ± 70	6540 (6360–6720)	Charcoal
SHERCI**	243	-695	126713	5425 ± 40	6235 (6035–6300)	Achenes
FW[#]	608	-580	126712	4340 ± 40	5440 (5327-5575)	Achenes
WTL**	350	-868	126719	5830 ± 40	6645 (6505–6740)	Achenes
WTL**	350	-868	126728	5905 ± 30	6720 (6665–6790)	Charcoal
WTCI**	184	-909	126718	5800 ± 35	6600 (6495–6710)	Achenes
TT	424	-404	126715	2315 ± 35	2340 (2160–2435)	Achenes
VIPP**	378	-830	126717	5790 ± 35	6590 (6495–6670)	Achenes
VICI**	198	-893	126716	5870 ± 35	6695 (6570–6785)	Achenes
BACHI	726	-705	126819	5085 ± 40	5820 (5740–5915)	Achenes
BACL**	257	-843	126709	5680 ± 35	6460 (6355–6560)	Achenes
BACPTC**	160	-788	126710	5475 ± 35	6280 (6200–6390)	Achenes
BACPTC**	160	-788	126721	5445 ± 35	6245 (6190–6300)	Charcoal

Table 3. Estimated vertical accretion rates for the marsh sites compared with Holocene average rates and twentieth century global rates of sea-level rise in cm yr^{-1}. [&]Mean accretion rate calculated only to -5.8 m MSL due to reversals below this depth. *Represents median of the 2 sigma-range (for error bars, see Figure 3).

Site and model type	Estimated range, mean, and sd of accretion for the entire peat column based on age-depth models	Estimated sea-level rise in the San Francisco Bay Estuary from 6000 yr ago to present (Atwater et al. 1977)	Twentieth century estimated rate of global sea-level rise (Church and White 2006)
BRI (spline fit)	(0.07 – 0.49), 0.18, 0.11	0.1 – 0.2	0.17 +/ 0.03
BACHI (spline fit)	(0.07 – 0.38), 0.16, 0.07	0.1 – 0.2	0.17 +/ 0.03
FW[&] (spline fit)	(0.03 – 0.16), 0.12, 0.03	0.1 – 0.2	0.17 +/ 0.03
TT (linear calculation using 3 data points)	Only two estimates available: 0.13* between 100 and 1210 cal yr BP 0.21* between 1210 and 2340 cal yr BP	0.1 – 0.2	0.17 +/ 0.03

Table 4. Bulk density and % organic matter (means ± standard deviations) for marsh island cores.		
Core	Mean bulk density (g cm^{-3})	Mean % organic matter
FW	0.14 ± 0.08	72 ± 19
BRI	0.31 ± 0.15	40 ± 18
BACHI	0.12 ± 0.05	76 ± 16
TT	0.23 ± 0.11	41 ± 13

Table 5. Relative contribution of OM_v and IM_v to soil volume in %. The remaining void space is filled by water and air.

Site	Mean OM_v (sd)	Mean IM_v (sd)
FW	6.15 (1.55)	2.3 (3.3)
BRI	9.25 (1.53)	8.45 (5.49)
BACHI	6.87 (1.99)	1.40 (1.67)
TT	7.17 (1.34)	5.77 (3.36)

LITERATURE CITED

Allen, J.R.L. 2000. Morphodynamics of Holocene salt marshes: a review sketch from the Atlantic and Southern North Sea coasts of Europe. Quaternary Science Reviews 19: 1155-1231.

Anisfield, S.C., M.J. Tobin, and G. Benoit. 1999. Sedimentation rates in flow-restricted and restored salt marshes in Long Island Sound. Estuaries 22:231-244.

Atwater, B. F. 1980. Attempts to correlate late Quaternary climatic records between San Francisco Bay, the Sacramento-San Joaquin Delta, and the Mokelumne River, California. Ph.D. Dissertation. University of Delaware, Newark, DE, USA.

Atwater, B.F. 1982. Geologic maps of the Sacramento-San Joaquin Delta, California. U.S. Geological Survey Miscellaneous Field Studies Map MF-1401, 20 map sheets, scale 1:24,000, Reston, Virginia, USA.

Atwater, B. F., and D. F. Belknap. 1980. Tidal-wetland deposits of the Sacramento-San Joaquin Delta, California. Pacific Coast Paleogeography Symposium 4:89–103.

Atwater, B.F., C.W. Hedel, and E.J. Helley. 1977. Late Quaternary depositional history, Holocene sea-level changes, and vertical crust movement, southern San Francisco Bay, California. U.S. Geological Survey Professional Paper 1014, 15 pp.

Bartberger, E.C. 1976. Sediment cores and sediment rates, Chincoteague Bay, Maryland and Virginia. Journal of Sedimentary Petrology 46: 326-336.

Bloom, A.L. 1964. Peat accumulation and compaction in a Connecticut coastal marsh. Journal of Sedimentary Petrology 34: 599-603..

Bricker-Urso S., S.W. Nixon, J.K. Cochran, D.J. Hirschberg, and C. Hunt. 1989. Accretion rates and sediment accumulation in Rhode Island marshes. Estuaries 12: 300-317.

Cahoon, D. R., P. F. Hensel, T. Spencer, D. J. Reed, K. L. McKee, and N. Saintilan. 2006. Coastal wetland vulnerability to sea-level rise: wetland elevation trends and process controls. p. 271-292. In J. T. A. Verhoeven, B. Beltman, R. Bobbink, and D. F. Whigham (eds.), Wetlands and Natural Resource Management, Ecological Studies Vol. 190, Springer-Verlag, Berlin, Germany.

California Department of Water Resources. 1995. Sacramento-San Joaquin Delta Atlas. Central District, Sacramento, CA, USA, http://baydeltaoffice.water.ca.gov/DeltaAtlas/index.cfm.

Church, J. A., and N. J. White. 2006. A 20th century acceleration in global sea-level rise. Geophysical Research Letters 33, L01602, doi:10.1029/2005GL024826.

DeLaune, R.D., R.H. Baumann, and J.G. Gosselink. 1983. Relationships among vertical accretion, coastal submergence, and erosion in a Louisiana Gulf coast marsh. Journal of Sedimentary Petrology 53: 147-157.

Deverel, S. J., and S. A. Rojstaczer. 1996. Subsidence of agricultural lands in the Sacramento-San Joaquin Delta, California: Role of aqueous and gaseous carbon fluxes. Water Resources Research 32:2359–2367.

Deverel, S. J., B. Wang, and S. Rojstaczer. 1998. Subsidence of organic soils, Sacramento-San Joaquin Delta, California. p. 489–502. In J. W. Borchers (ed.) Land Subsidence Case Studies and Current Research. Association of Engineering Geologists Special Publication No. 8.

Deverel, S. J.and Leighton, David A., 2008, Subsidence causes and rates in the Sacramento-San Joaquin Delta and Suisun Marsh. San Francisco Estuary and Water Science, in press.

Drexler, J. Z., C. S. de Fontaine, and D. L. Knifong. 2007. Age determination of the remaining peat in the Sacramento-San Joaquin Delta, California, USA. U.S. Geological Survey Open File Report 2007-1303. 2 pp.

Drexler, J. A., C. S. de Fontaine, and S. J. Deverel. 2009. The legacy of wetland drainage on the remaining peat in the Sacramento - San Joaquin Delta, California, USA. Wetlands in press.

Enzel, Y. D. R. Cayan, R. Y. Anderson, and S. G. Wells. 1989. Atmospheric circulation during Holocene lake stands in the Mojave Desert: Evidence of regional climate change. Nature 341: 44-47.

Gilbert, G. K., 1917. Hydraulic-mining debris in the Sierra Nevada. U.S. Geological Survey, Professional paper 105, U.S. Government Printing Office, Washington, DC, USA.

Goman, M. and Wells, L. 2000. Trends in river flow affecting the northeastern reach of the San Francisco Bay Estuary over the past 7000 years. Quaternary Research 54: 206-217.

Givelet, N., G. Le Roux, A. Cheburkin, B. Chen, J. Frank, M. Goodsite, H. Kempter, M. Krachler, T. Noernberg, N. Rausch, S. Rheinberger, F. Roos-Barraclough, A. Sapkota, C. Scholz, and W. Shotyk. 2004. Suggested protocol for collecting, handling and preparing peat cores and peat

samples for physical, chemical, mineralogical and isotopic analyses. Journal of Environmental Monitoring 6:481–492.

Hatton, R.S., R..D. DeLaune, and W.H. Patrick, Jr. 1983. Sedimentation, accretion, and subsidence in marshes of Barataria Basin, Louisiana. Limnology and Oceanography 28: 494-502.

Heegaard, E., H.J.B. Birks, and R.J. Telford. 2005. Relationships between calibrated ages and depth in stratigraphical sequences: an estimation procedure by mixed-effect regression. The Holocene 15: 612-618.

Hensel, P.F., J.W. Day, Jr., and D. Pont. 1998. Wetland vertical accretion and soil elevation change in the Rhone River Delta, France: the importance of riverine flooding. Journal of Coastal Research 15(3): 668-681.

Hickman, J. C. (ed.). 1993. The Jepson Manual. University of California Press, Berkeley, CA, USA. 1400 pp.

Hillel, D. 1998. Environmental soil physics: fundamentals, applications, and environmental considerations. Elsevier Science and Technology Books, San Diego, CA, 771 pp..

Ingebritsen, S. E., and M. E. Ikehara. 1999. Sacramento-San Joaquin Delta: the sinking heart of the state. p. 83–94. In D. Galloway, D. R. Jones, and S. E. Ingebritsen (eds.) Land Subsidence in the United States. Circular 1182. U.S. Geological Survey, Reston, VA, USA.

Kaye, C.A. and E.S. Barghoorn. 1964. Late Quaternary sea level and crustal rise at Boston, Massachusetts with notes on the autocompaction of peat. Geological Society of America Bulletin 75: 63-80.

Keene, H.W. 1971. Postglacial submergence and salt marsh evolution in New Hampshire. Maritime Sediments 7:64-68.

Khan, H. and G.S. Brush. 1994. Nutrient and metal accumulation in a freshwater tidal marsh. Estuaries 17: 345-360

LaMarche Jr., V. 1973. Holocene climatic variations inferred from treeline fluctuations in the White Mountains California. Quaternary Research 3: 632:660.

Liu, K.B., S. Sun, and X. Jiang. 1992. Environmental change in the Yangtze River delta since 12,000 years BP. Quaternary Research 38: 32-45.

Meehl, G.A., T.F. Stocker, W.D. Collins, P. Friedlingstein, A.T. Gaye, J.M. Gregory, A. Kitoh, R. Knutti, J.M. Murphy, A. Noda, S.C.B. Raper,I.G. Watterson, A.J. Weaver and Z.-C. Zhao, 2007: Global Climate Projections. *In*: Climate Change 2007: The Physical Science Basis.Contribution of Working Group I to the Fourth Assessment Report of the Intergovernmental Panel on Climate Change [Solomon, S.,D. Qin, M. Manning, Z. Chen, M. Marquis, K.B. Avery, M. Tignor and H.L. Miller (eds.)]. Cambridge University Press, Cambridge, United Kingdom and New York, NY, USA.

Merrill, J.Z. and J.C. Cornwell. 2000. The role of oligohaline marshes in estuarine nutrient cycling, pp. 425-441. In: M. Weinstein and D.A. Kreeger (eds.), Concepts and Controversies in Tidal Marsh Ecology. Kluwer Press, Dordrecht, The Netherlands.

Miller, R.L., L. Hastings, R. Fujii. 1997. Hydrologic treatments affect gaseous carbon loss from organic soils, Twitchell Islands, California, October 1995-December 1997. U.S. Geological Survey Water-Resources Investigations Report 00-4042, Sacramento, California, USA, 21pp.

Mitsch, W. J., and J. G. Gosselink. 2000. Wetlands, third edition. John Wiley & Sons, Inc., New York, NY, USA.

Mount, J., and R. Twiss. 2005. Subsidence, sea level rise, seismicity in the Sacramento-San Joaquin Delta. San Francisco Estuary and Watershed Science Vol. 3, Issue 1 (March 2005), Article 5. http://repositories.cdlib.org/jmie/sfews/vol3/iss1/art5

Neubauer, S.C. I.C. Anderson, J.A. Constantine, and S.A. Kuehl. 2002. Sediment deposition and accretion in a mid-Atlantic (USA) tidal freshwater marsh. Estuarine, Coastal, and Shelf Science 54: 713-727.

Neubauer, S.C. 2008. Contributions of mineral and organic components to tidal freshwater marsh accretion. Estuarine, Coastal and Shelf Science 78:78-88.

Odum, W.E. 1988. Comparative ecology of tidal freshwater and salt marshes. Annual Review of Ecology and Systematics 19: 147-176.

Okruszko, H. 1971. Determination of specific gravity of hydrogenic soils on the basis of their mineral particles content. Wiadomosci Instytutu Melioracji i Uzytkow Zielonych X(1): 47-54.

Orr, M., S. Crooks, and P.B. Williams. 2003. Will restored tidal marshes be sustainable? San Francisco Estuary and Watershed Science Issue 1, Article 5. http://respositories.cdlib.org/jmie/sfews/vol1/iss1/art5

Penland, S., and K. E. Ramsey. 1990. Relative sea-level rise in Louisiana and the Gulf of Mexico: 1908–1988. Journal of Coastal Research 6:323–342.

Pizzuto, J.E. and A. E. Schwendt. 1997. Mathematical modeling of autocompaction of a Holocene transgressive valley-fill deposit, Wolfe Glade, Delaware. Geology 25:57-60.

Prokopovich, N. P. 1985. Subsidence of peat in California and Florida. Bulletin of the Association of Engineering Geologists 22:395–420.

Redfield, A.C. 1967. Postglacial change in sea level in the western north Atlantic Ocean. Science 157: 687-690.

Reed, D.J. 2000. Coastal biogeomorphology: an integrated approach to understanding the evolution, morphology, and sustainability of temperate coastal marshes. pp. 347-361. In: Hobbie, J.E. (ed.), Estuarine Science: a synthetic approach to research and practice. Island Press, Washington, D.C.

Reed, D.J. 2002a. Sea-level rise and coastal marsh sustainability: geological and ecological factors in the Mississippi delta plain. Geomorphology 48: 233-243.

Reed, D.J. 2002b. Understanding tidal marsh sedimentation in the Sacramento-San Joaquin Delta, California. Journal of Coastal Research SI 36: 605-611.

Reimer, P. J., M. G. L. Baillie, E. Bard, A. Bayliss, J. W. Beck, C. J. H. Bertrand, P. G. Blackwell, C. E. Buck, G. S. Burr, K. B. Cutler, P. E. Damon, R. L. Edwards, R. G. Fairbanks, M. Friedrich, T. P. Guilderson, A. G. Hogg, K. A. Hughen, B. Kromer, G. McCormac, S. Manning, C. B. Ramsey, R. W. Reimer, S. Remmele, J. R. Southon, M. Stuiver, S. Talamo, F. W. Taylor, J. van der Plicht, and C. E. Weyhenmeyer. 2004. IntCal04 terrestrial radiocarbon age calibration, 0-26 cal kyr BP. Radiocarbon 46:1029–1058.

Robinson, S.D. and Moore, T.R. 1999. Carbon and peat accumulation over the past 1200 years in a landscape with discontinuous permafrost, northwestern Canada. Global Biogeochemical Cycles 13(2): 591-601.

Rojstaczer, S., and S. J. Deverel. 1993. Time dependence in atmospheric carbon inputs from drainage of organic soils. Geophysical Research Letters 20:1383–1386.

Rojstaczer, S., and S. J. Deverel. 1995. Land subsidence in drained histosols and highly organic mineral soils of California. Soil Science Society of America Journal 59:1162–1167.

Rojstaczer, S. A., R. E. Hamon, S. J. Deverel, and C. A. Massey, 1991. Evaluation of selected data to assess the causes of subsidence in the Sacramento-San Joaquin Delta, California. U.S. Geological Survey, Sacramento, CA, USA. Open-File Report 91-0193, 16 pp.

Sawai, Y., N. Hiroo and Y. Yasuda. 2002. Fluctuations in relative sea-level during the past 3000 yr in the Onnetoh estuary, Hokkaido, northern Japan. Journal of Quaternary Science 17: 607-622.

Schoellhamer, D., Wright, S., Drexler, J.Z., Stacey, M. Sedimentation Conceptual Model. 2007. White Paper for the California Bay/Delta Science Program, 35 pp.

Service, R.J. 2007. Delta blues, California style. Science 317: 442-445.

Shennan, I., A. J. Long, M. M. Rutherford, J. B. Innes, F. M. Green, J. R. Kirby, and K. J. Walker. 1998. Tidal marsh stratigraphy, sea-level change and large earthquake—II: submergence events during the last 3500 years at Netarts Bay, Oregon, U.S.A. Quaternary Science Reviews 17: 365-393.

Shlemon, R.J. and E.L. Begg. 1975. Late Quaternary evolution of the Sacramento-San Joaquin Delta, California. pp. 259-266 In R.P. Suggate and M.M. Creswell (eds.) Quaternary Studies. The Royal Society of New Zealand, Wellington, New Zealand.

Stanley, D. J. and A. G. Warne. 1994. Worldwide initiation of Holocene marine deltas by deceleration of sea-level rise. Science 265:228-231.

Stevenson, J.C., M.S. Kearney, E.C. Pendleton. 1986. Vertical accretion rates in marshes with varying rates of sea-level rise. pp. 241-260. In: Woldf, D. (ed.), Estuarine Variability, Academic Press, New York, USA.

Stine, S. 1990. Late Holocene fluctuations of Mono Lake, eastern California. Palaeogeography, Palaeoclimatology, Palaeoecology 78: 333-381.

Stuiver, M., and P. J. Reimer. 1993. Extended ^{14}C data base and revised CALIB 3.0 ^{14}C age calibration program. Radiocarbon 35:215–230.

Temmerman, S., G. Govers, S. Wartel, and P. Meire. 2004. Modelling estuarine variations in tidal marsh sedimentation: response to changing sea level and suspended sediment concentrations. Marine Geology 212: 1-19.

Turetsky, M.R., S.W. Manning, and R.K. Wieder. 2004. Dating recent peat deposits. Wetlands 24: 324-356.

Thompson, J. 1957. The settlement geography of the Sacramento-San Joaquin Delta, California. Ph.D. Dissertation. Stanford University, Stanford, CA, USA.

Tornqvist, T.E., A.F.M. De Jong, W.A. Oosterbaan, and K. Van der Borg. 1992. Accurate dating or organic deposits by AMS 14C measurement of macrofossils. Radiocarbon 34: 566-577.

Tornqvist, TE, JL Gonzalez, LE Newsom, K van der Borg, and AFM de Jong, CW Kurnik. 2004. Deciphering Holocene sea-level history on the US Gulf Coast: a high-resolution record from the Mississippi Delta. GSA Bulletin 116: 1026-1039.

Tornqvist, TE, SJ Bick, K van der Borg, and AFM de Jong. 2006. How stable is the Mississippi Delta? Geology 34: 697-700.

United States Department of Agriculture Soil Conservation Service. 2006. Keys to soil taxonomy. Tenth edition. ftp://ftp-fc.sc.egov.usda.gov/NSSC/Soil_Taxonomy/keys/keys.pdf

van Heteren, S. and O. van de Plassche. 1997. Influence of relative sea-level change and tidal inlet development on barrier-spit stratigraphy, Sandy Neck, Massachusetts. Journal of Sedimentary Research 67: 350-363.

Weber-Band 1998. Neotectonics of the Sacramento-San Joaquin Delta area, east central Coast Ranges, California. Ph.D. thesis, University of California, Berkeley.

Wells, L. E. 1995. Radiocarbon dating of Holocene tidal marsh deposits: Applications to reconstructing relative sea level changes in the San Francisco estuary. p. 3.95–3.102. In J. S. Noller, W. R. Lettis, and J. M. Sowers (eds.) Quaternary Geochronology and Paleoseismology. Nuclear Regulatory Commission, Washington, DC, USA

West, G. J. 1977. Late Holocene vegetation history of the Sacramento-San Joaquin Delta, California. Unpublished report prepared for the California Department of Water Resources under

Interagency Agreement B-50 173 by the Cultural Heritage Section of the California Department of Parks and Recreation.

Witter, R.C., H.M. Kelsey, and E. Hemphill-Haley. 2003. Great Cascadia earthquakes and tsunamis of the past 6700 years, Coquille River estuary, southern coastal Oregon. Geological Society of America Bulletin 115: 1289-1306.

Wright, H. E., Jr. 1991. Coring tips. Journal of Paleolimnology 6:37–49.

Wright, S.A., and Schoellhamer, D.H., 2004. Trends in the Sediment Yield of the Sacramento River, California, 1957 – 2001: San Francisco Estuary and Watershed Science. v. 2, no. 2, article 2. http://repositories.cdlib.org/jmie/sfews/vol2/iss2/art2

Wright, S.A., and Schoellhamer, D.H., 2005. Estimating sediment budgets at the interface between rivers and estuaries with application to the Sacramento–San Joaquin River Delta: Water Resources Research, v. 41, W09428, doi:10.1029/2004WR003753.

Yang, S.L., I.M. Belkin, A.I. Belina, Q.Y. Zhao, J. Zhu, P.X. Ding. 2003. Delta response to decline in sediment supply from the Yangtze River: evidence of the recent four decades and expectations for the next half-century: Estuarine, Coastal and Shelf Science 57: 689-699.

Zoltai, S.C. and J.D. Johnson. 1984. Development of a treed bog island in a minerotrophic fen. Canadian Journal of Botany 63: 1076-1085.

Figure Legends

Figure 1. Location and site map of the Sacramento-San Joaquin Delta, California, U.S.A. The legend contains all coring locations and names of each the farmed and marsh sites in the study.

Figure 2. Radiocarbon data in calibrated years before present (cal yr BP) for all cores presented by (a) depth below surface and (b) depth relative to local mean sea level (MSL). Each data point is the median probability of the 2-sigma range. The x-axis error bars encompass the minimum and maximum 2-sigma range. Y-axis error bars are not shown in part (a) because error is on the order of a few millimeters for this study. Error bars for depth relative to mean sea level in part (b) incorporates the error estimates from the RTK GPS survey and Atwater et al. (1977). Radiocarbon dates from Shlemon and Begg (1975) and Atwater et al. (1977) are shown separately in plots (a) and (b) due to their use of depth from surface vs. mean sea level, respectively, as reference points for elevation. Details for each radiocarbon sample are provided in Appendix 1.

Figure 3. Diagnostic plots for the cubic smooth spline regression (residuals vs. fitted values, square root of absolute residuals vs. fitted, observed vs. fitted, and a qq-normplot) and spline fit models for (a) FW (n=9), (b) BRI (n=24), and (c) BACHI (n=12). A polynomial trend line, (d), is shown for TT. The model for FW ends at -5.8 m relative to MSL because of major age reversals below this depth. The plot for BRI contains raw data from both Core 4 and Core 5 at the site.

Figure 4. Calculated porosity vs. elevation relative to MSL (m) at FW. The porosity values within the oval were used to assess the degree of autocompaction in the peat.

Figure 5. Estimated yearly vertical accretion rates calculated from the spline fit models for FW, BRI, and BACHI.

Figure 6. Relative contribution of inorganic vs. organic matter to soil volume for each marsh site. The remaining void space is filled with water and/or air.

Figure 1.

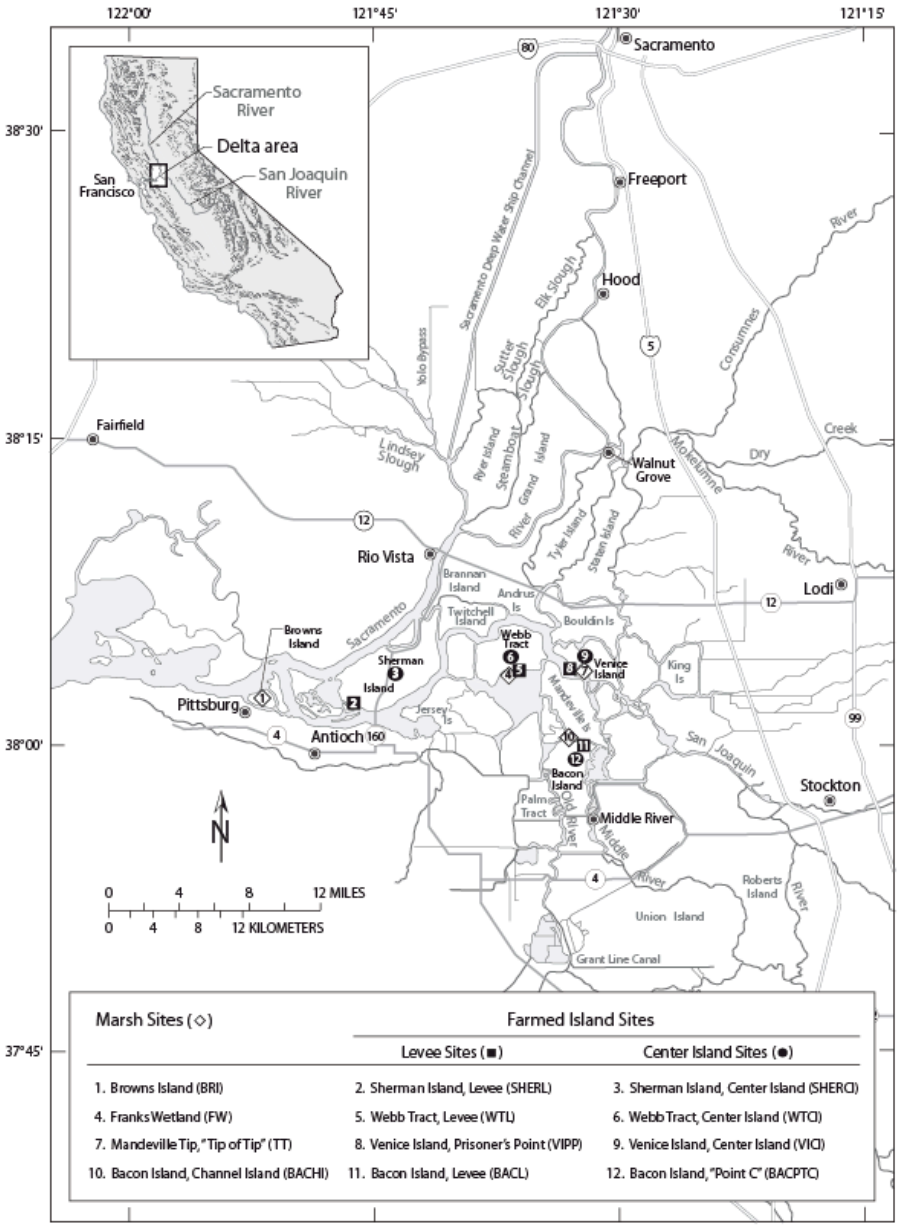
122°00'
121°45'
121°30'
121°15'
38°30'
38°15'
38°00'
37°45'
Sacramento River
Delta area
San Joaquin River
San Francisco
Sacramento
Freeport
Hood
Fairfield
Walnut Grove
Rio Vista
Lodi
Stockton
Pittsburg
Antioch
Middle River
Browns Island
Sherman Island
Webb Tract
Venice Island
Bacon Island
Union Island
Roberts Island
Grant Line Canal
Sacramento Deep Water Ship Channel
Elk Slough
Sutter Slough
Steamboat Slough
Lindsey Slough
Yolo Bypass
Mokelumne River
Dry Creek
Consumnes River
Tyler Island
Staten Island
Brannan Island
Andrus Is
Twitchell Island
Bouldin Is
King Is
Jersey Is
Mandeville Is
San Joaquin River
Palmas Tract
Old River
Middle River
0 4 8 12 MILES
0 4 8 12 KILOMETERS
Marsh Sites (◇)
Farmed Island Sites
Levee Sites (■)
Center Island Sites (●)
1. Browns Island (BRI)
2. Sherman Island, Levee (SHERL)
3. Sherman Island, Center Island (SHERCI)
4. Franks Wetland (FW)
5. Webb Tract, Levee (WTL)
6. Webb Tract, Center Island (WTCI)
7. Mandeville Tip, "Tip of Tip" (TT)
8. Venice Island, Prisoner's Point (VIPP)
9. Venice Island, Center Island (VICI)
10. Bacon Island, Channel Island (BACHI)
11. Bacon Island, Levee (BACL)
12. Bacon Island, "Point C" (BACPTC)

Figure 2a.

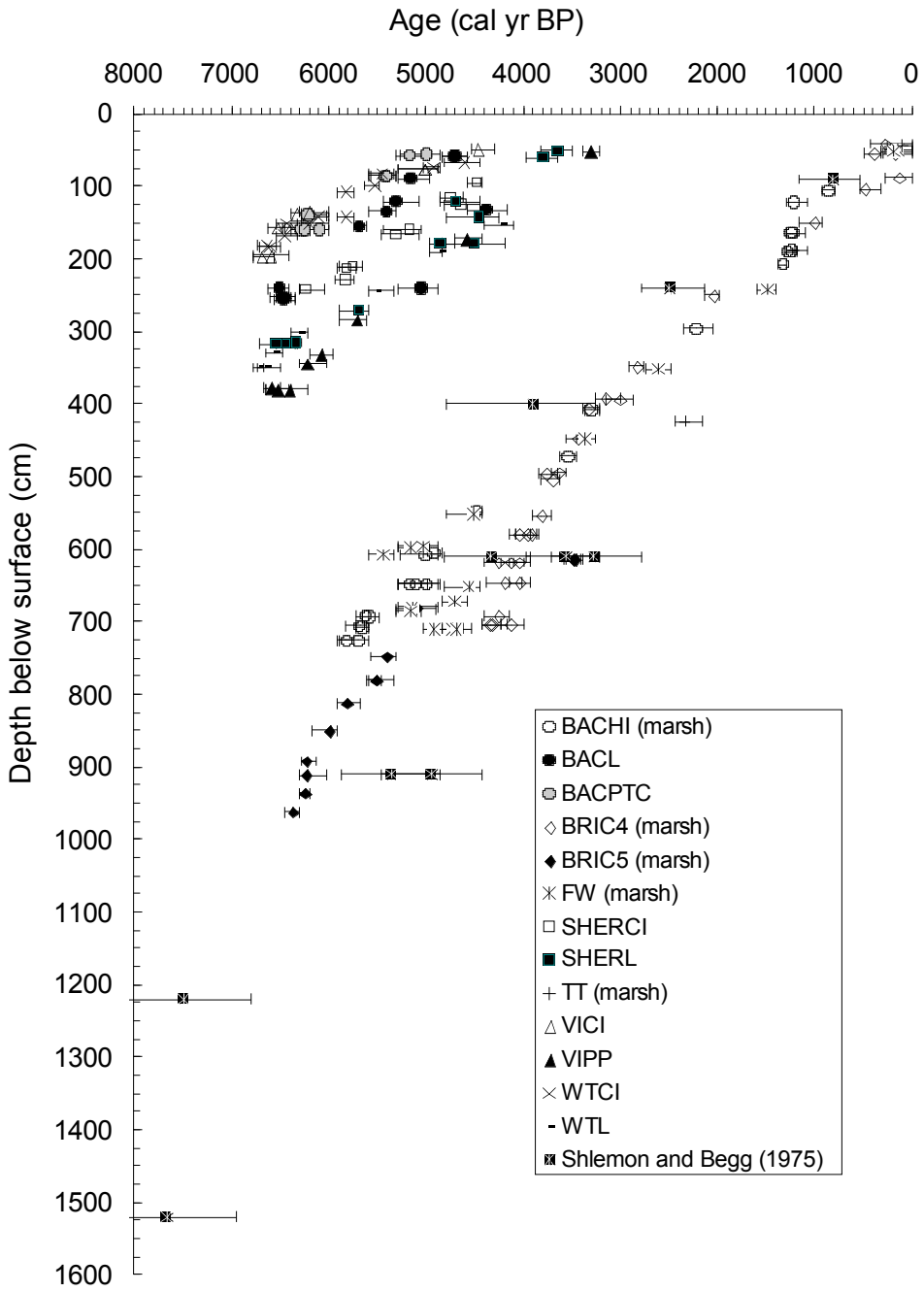
Age (cal yr BP)
8000
7000
6000
5000
4000
3000
2000
1000
0
Depth below surface (cm)
0
100
200
300
400
500
600
700
800
900
1000
1100
1200
1300
1400
1500
1600
BACHI (marsh)
BACL
BACPTC
BRIC4 (marsh)
BRIC5 (marsh)
FW (marsh)
SHERCI
SHERL
TT (marsh)
VICI
VIPP
WTCI
WTL
Shlemon and Begg (1975)

Figure 2b.

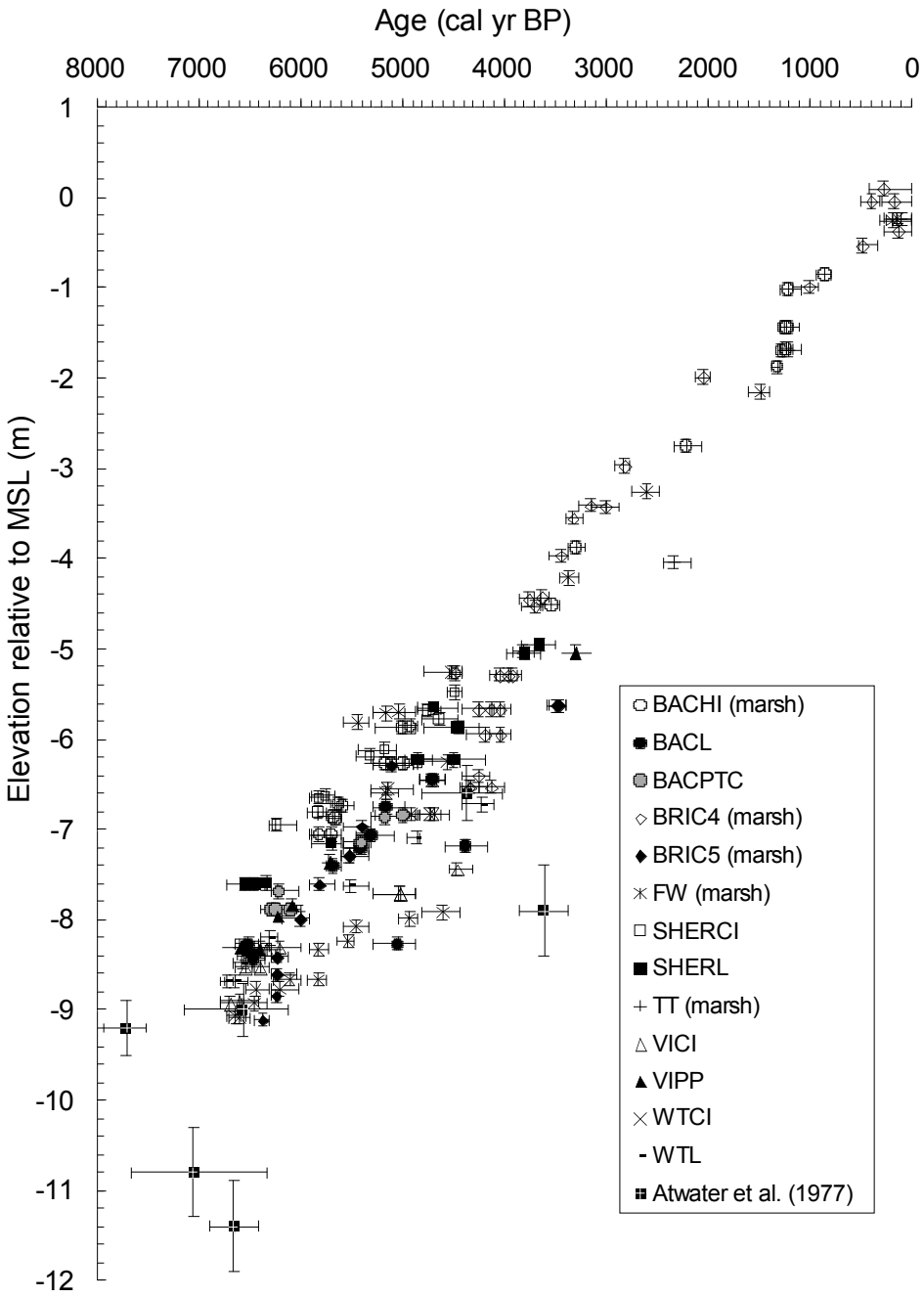
Age (cal yr BP)
8000
7000
6000
5000
4000
3000
2000
1000
0
Elevation relative to MSL (m)
1
0
-1
-2
-3
-4
-5
-6
-7
-8
-9
-10
-11
-12
BACHI (marsh)
BACL
BACPTC
BRIC4 (marsh)
BRIC5 (marsh)
FW (marsh)
SHERCI
SHERL
TT (marsh)
VICI
VIPP
WTCI
WTL
Atwater et al. (1977)

Figure 3.

(a)

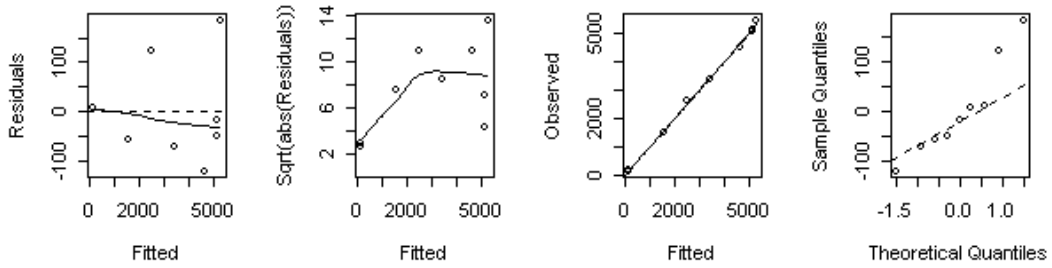
Residuals
Fitted
Sqrt(abs(Residuals))
Fitted
Observed
Fitted
Sample Quantiles
Theoretical Quantiles

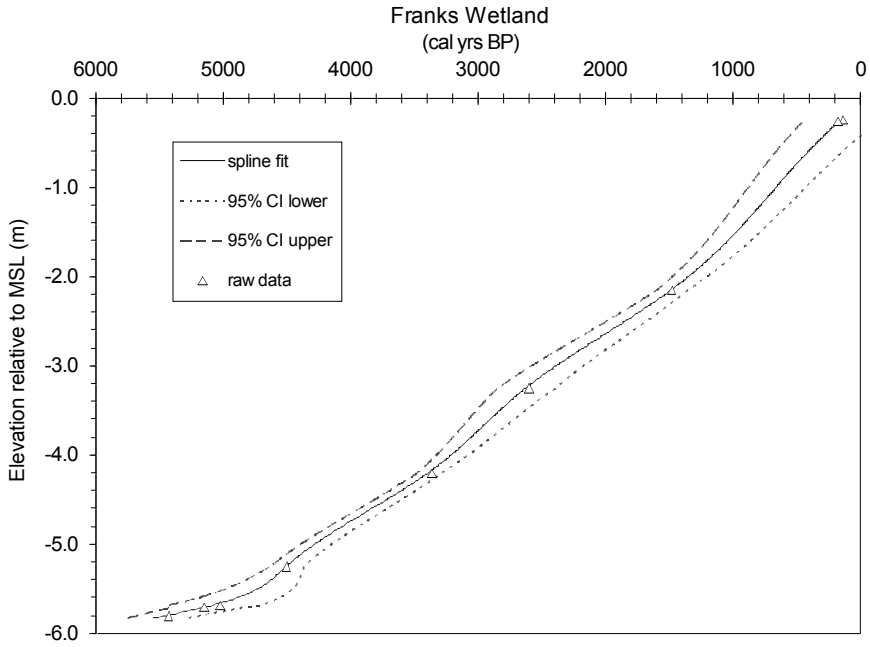
Franks Wetland
(cal yrs BP)
Elevation relative to MSL (m)
spline fit
95% CI lower
95% CI upper
raw data

(b)

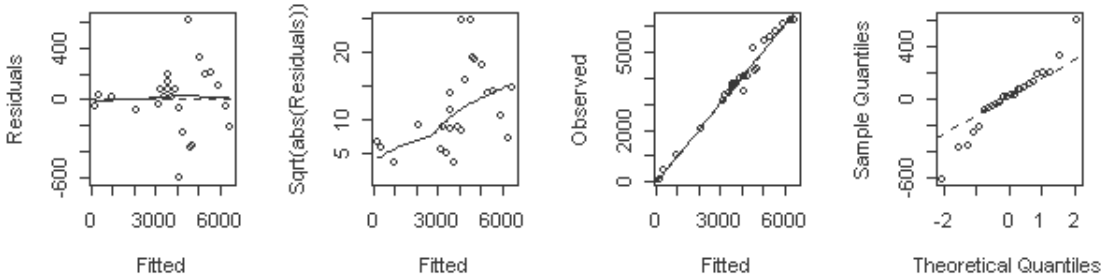
Residuals
Fitted
Sqrt(abs(Residuals))
Fitted
Observed
Fitted
Sample Quantiles
Theoretical Quantiles

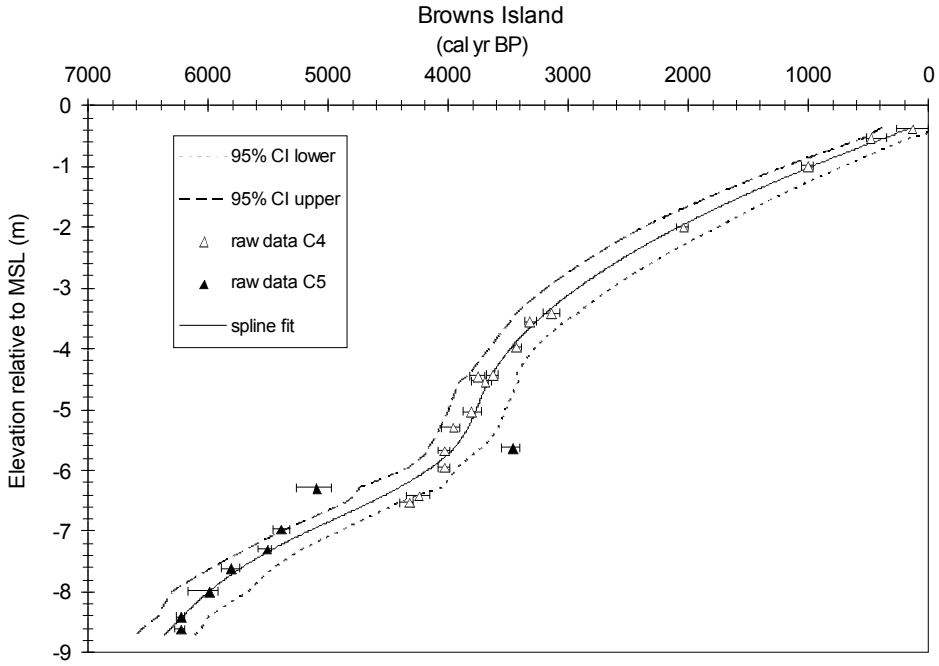
Browns Island
(cal yr BP)
Elevation relative to MSL (m)
95% CI lower
95% CI upper
raw data C4
raw data C5
spline fit

(c)

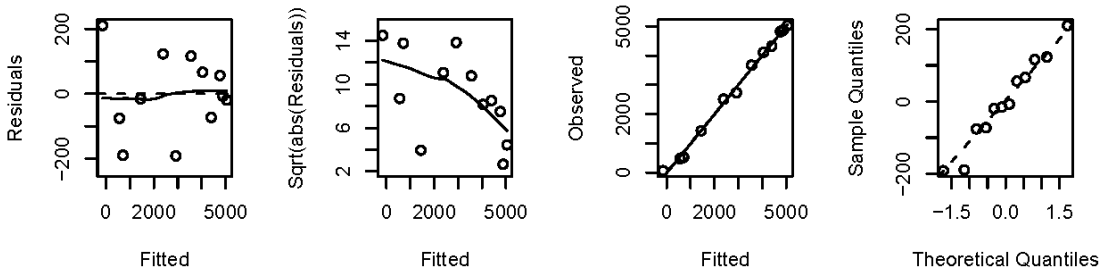
Residuals
Fitted
Sqrt(abs(Residuals))
Fitted
Observed
Fitted
Sample Quantiles
Theoretical Quantiles

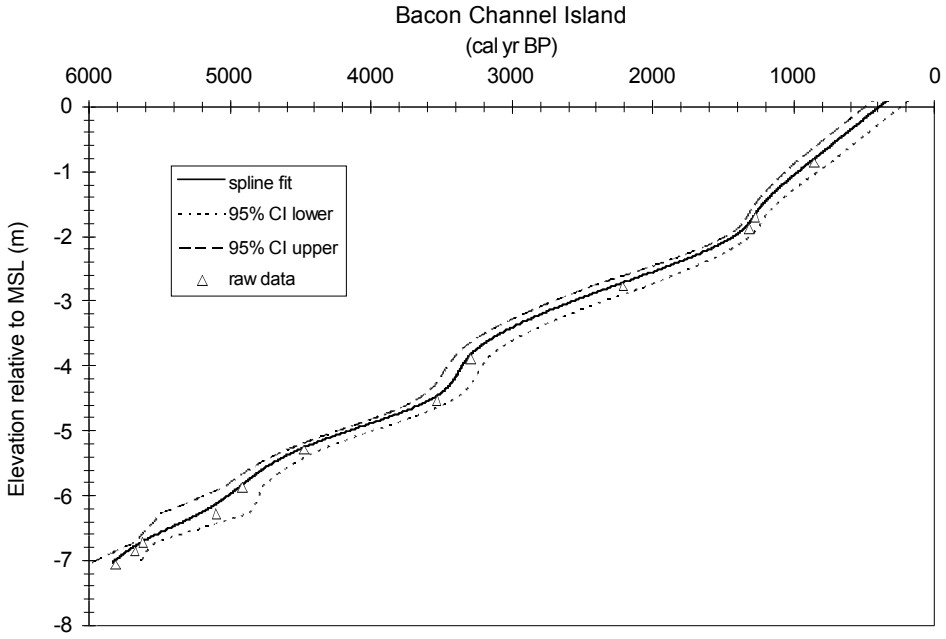
Bacon Channel Island
(cal yr BP)
Elevation relative to MSL (m)
spline fit
95% CI lower
95% CI upper
raw data

(d)

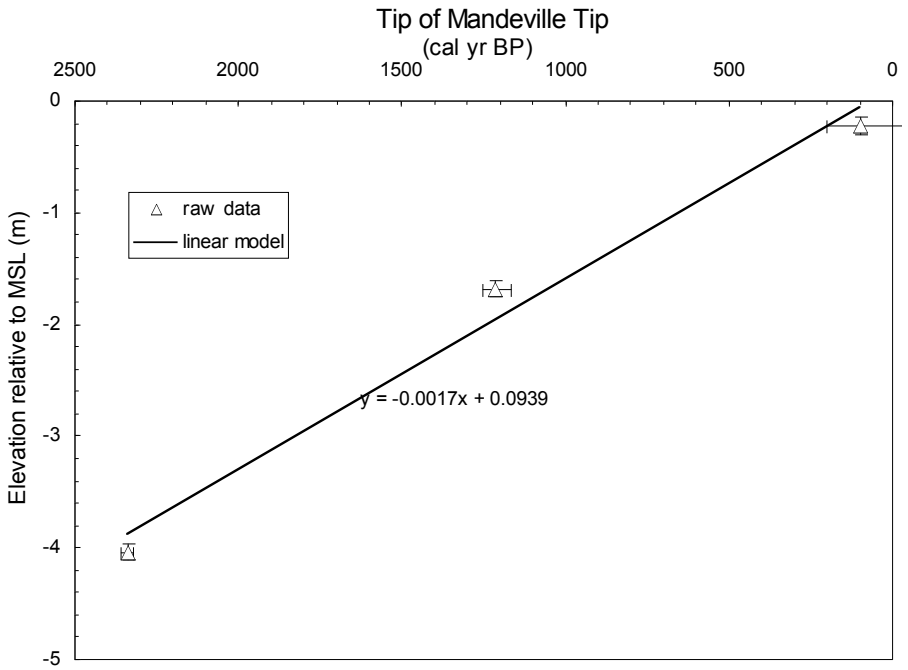
Tip of Mandeville Tip
(cal yr BP)
2500
2000
1500
1000
500
0
0
-1
-2
-3
-4
-5
Elevation relative to MSL (m)
raw data
linear model
y = -0.0017x + 0.0939

Figure 4.

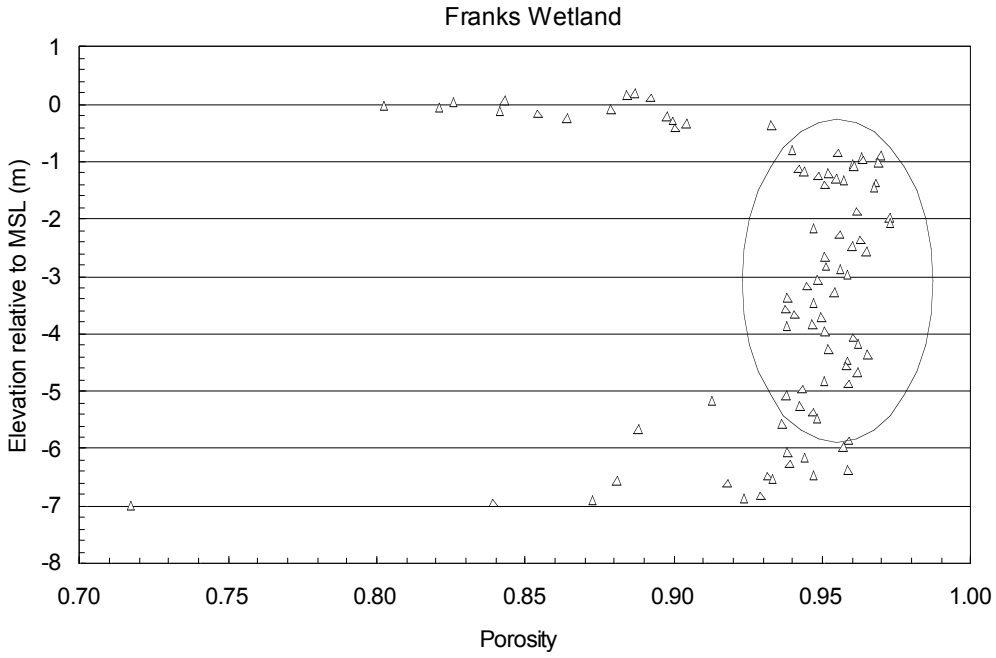
Franks Wetland
1
0
-1
-2
-3
-4
-5
-6
-7
-8
Elevation relative to MSL (m)
0.70
0.75
0.80
0.85
0.90
0.95
1.00
Porosity

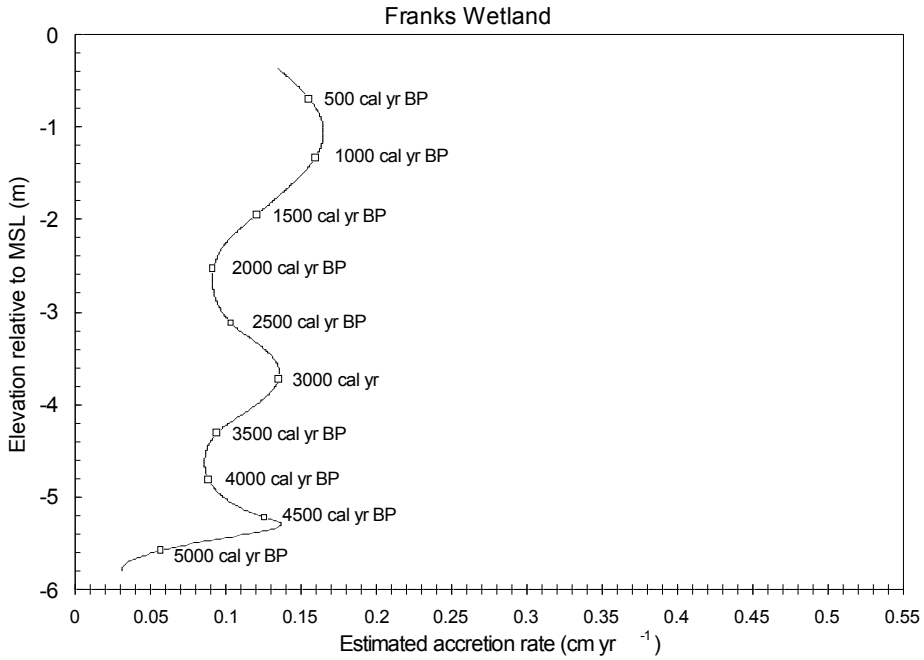
Franks Wetland
Elevation relative to MSL (m)
0
-1
-2
-3
-4
-5
-6
500 cal yr BP
1000 cal yr BP
1500 cal yr BP
2000 cal yr BP
2500 cal yr BP
3000 cal yr
3500 cal yr BP
4000 cal yr BP
4500 cal yr BP
5000 cal yr BP
0
0.05
0.1
0.15
0.2
0.25
0.3
0.35
0.4
0.45
0.5
0.55
Estimated accretion rate (cm yr -1)

Figure 5.

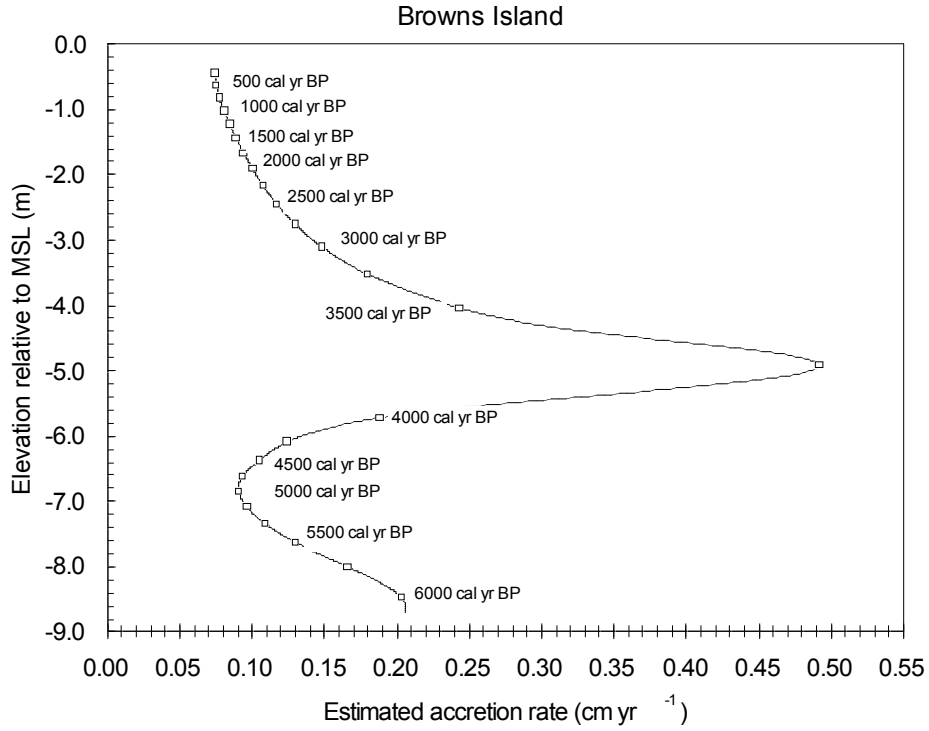
Browns Island
Elevation relative to MSL (m)
0.0
-1.0
-2.0
-3.0
-4.0
-5.0
-6.0
-7.0
-8.0
-9.0
500 cal yr BP
1000 cal yr BP
1500 cal yr BP
2000 cal yr BP
2500 cal yr BP
3000 cal yr BP
3500 cal yr BP
4000 cal yr BP
4500 cal yr BP
5000 cal yr BP
5500 cal yr BP
6000 cal yr BP
0.00
0.05
0.10
0.15
0.20
0.25
0.30
0.35
0.40
0.45
0.50
0.55
Estimated accretion rate (cm yr -1)

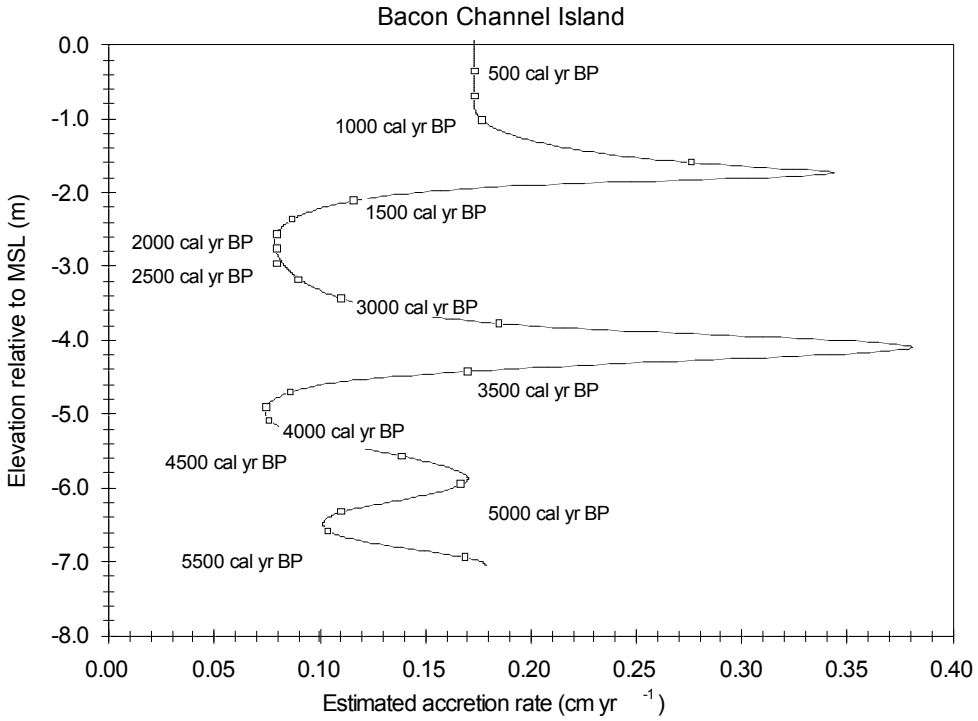
Bacon Channel Island
0.0
-1.0
-2.0
-3.0
-4.0
-5.0
-6.0
-7.0
-8.0
Elevation relative to MSL (m)
500 cal yr BP
1000 cal yr BP
1500 cal yr BP
2000 cal yr BP
2500 cal yr BP
3000 cal yr BP
3500 cal yr BP
4000 cal yr BP
4500 cal yr BP
5000 cal yr BP
5500 cal yr BP
0.00
0.05
0.10
0.15
0.20
0.25
0.30
0.35
0.40
Estimated accretion rate (cm yr -1)

Figure 6.

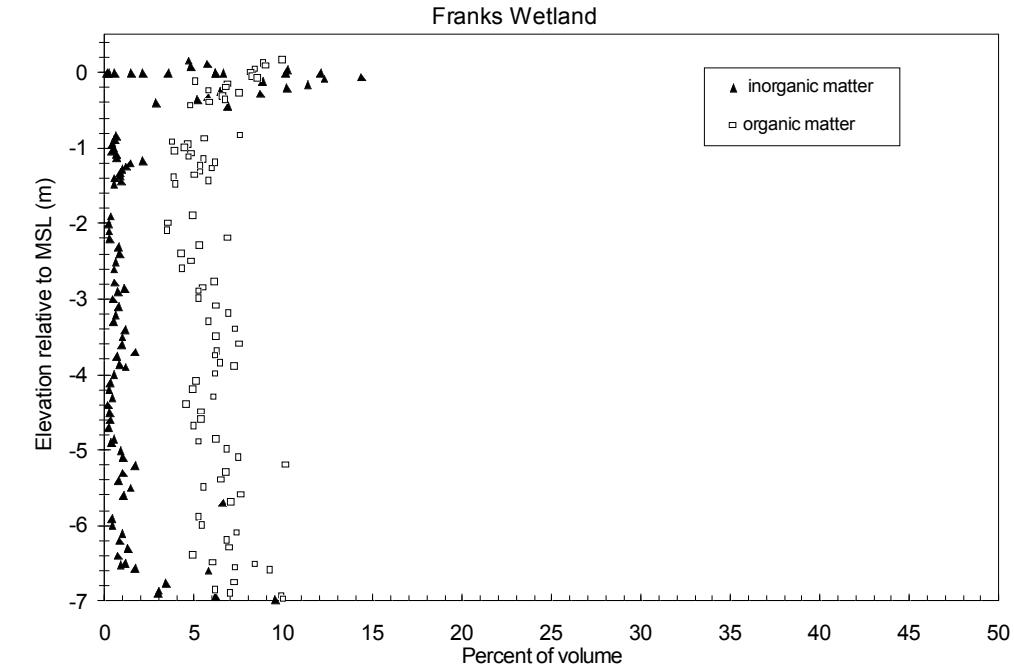
Franks Wetland
inorganic matter
organic matter
Elevation relative to MSL (m)
0
-1
-2
-3
-4
-5
-6
-7
0
5
10
15
20
25
30
35
40
45
50
Percent of volume

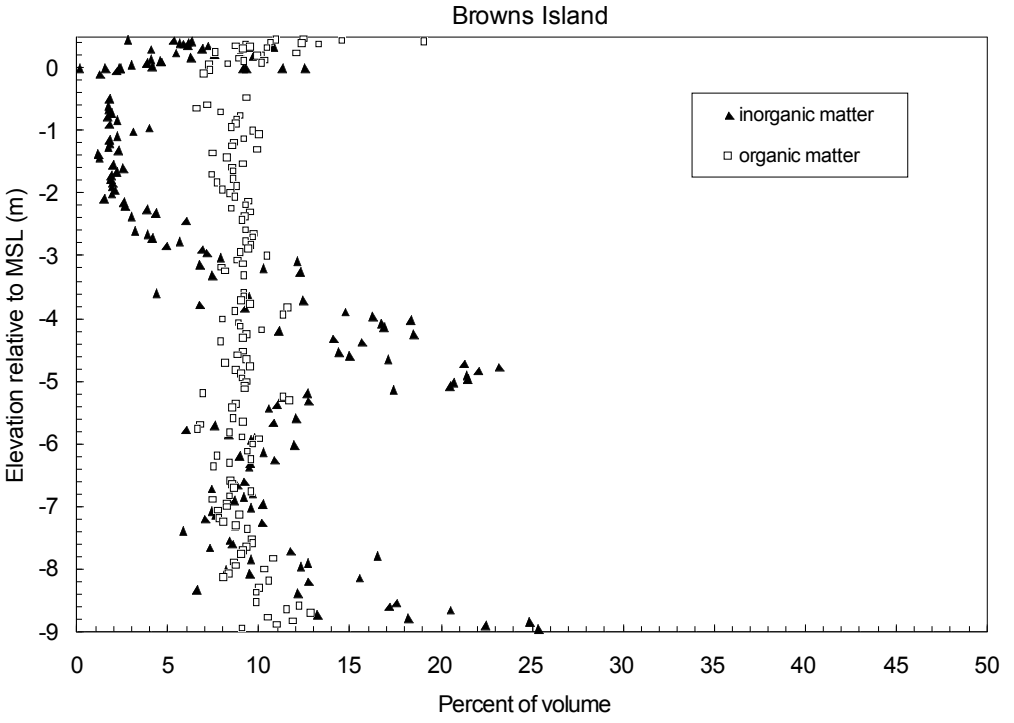
Browns Island
inorganic matter
organic matter
Elevation relative to MSL (m)
0
-1
-2
-3
-4
-5
-6
-7
-8
-9
0
5
10
15
20
25
30
35
40
45
50
Percent of volume

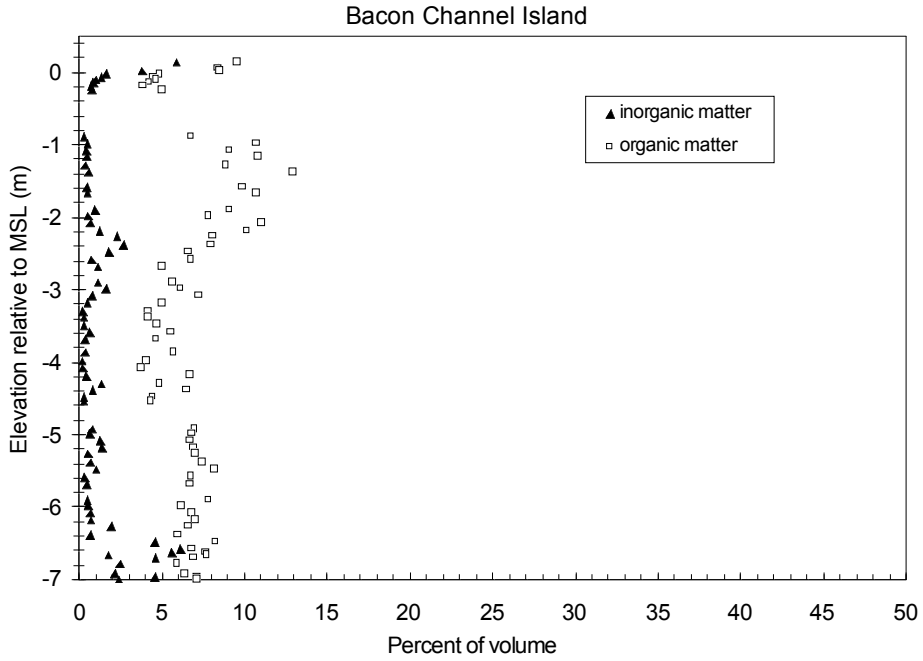
Bacon Channel Island
inorganic matter
organic matter
Elevation relative to MSL (m)
0
-1
-2
-3
-4
-5
-6
-7
0
5
10
15
20
25
30
35
40
45
50
Percent of volume

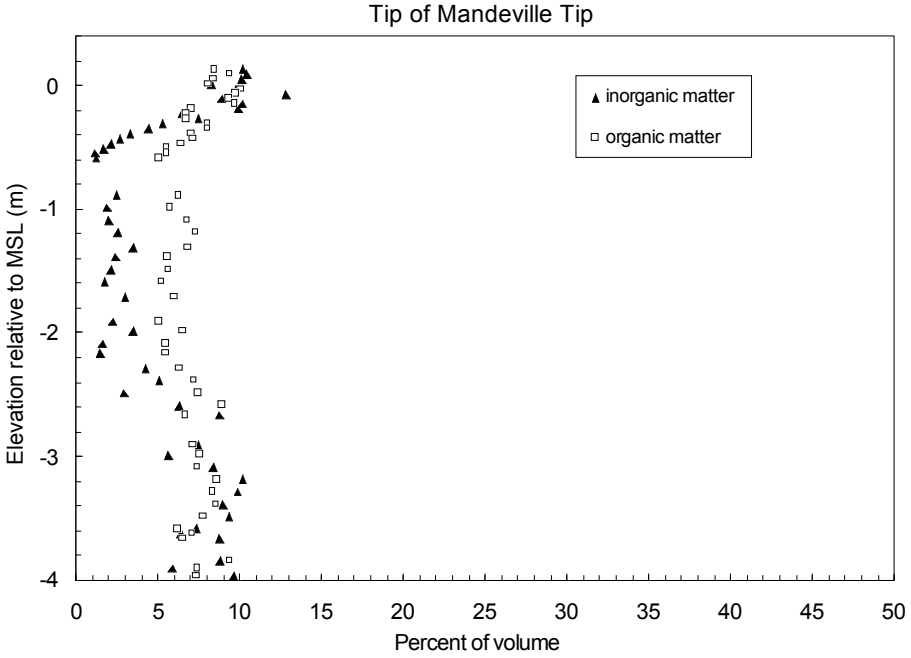
Tip of Mandeville Tip
inorganic matter
organic matter
Elevation relative to MSL (m)
0
-1
-2
-3
-4
0
5
10
15
20
25
30
35
40
45
50
Percent of volume

Appendix 1. Data for ^{14}C samples from all coring sites in this study. In addition, data from Shlemon and Begg (1975) collected across an east-west transect in the Delta and data from Atwater et al. (1977) collected in San Francisco Bay are included. *Represents depths for which elevations are depths below surface and not relative to mean sea level (m). Granular fragments are unidentified organic material that may be fern spores.

CAMS Lab Code	Site, Core, and Sample ID	Sample Thickness (cm)	Sample Bottom Elevation (MSL in m)	^{14}C age (^{14}C yr BP)	2-sigma ^{14}C Error (^{14}C yr BP)	Median probability of 2-sigma Range (cal yr BP)	Sample Material
130030	BACHIC1D2-4B	2	-0.85	960	70	857	Charcoal
128459	BACHIC1D2-12A	2	-1.01	1265	70	1214	Wood
128460	BACHIC1D2-33A	2	-1.43	1315	80	1249	Achenes
130031	BACHIC1D2-45A	2	-1.67	1290	60	1235	Achenes
128461	BACHIC1D2-46A	2	-1.69	1340	60	1279	Achenes
128462	BACHIC1D3-5B	2	-1.87	1415	70	1322	Wood
136897	BACHIC1D3-49A	2	-2.75	2200	120	2217	Plant fragment
136898	BACHIC1D5-5A	2	-3.87	3075	70	3298	Plant fragment
136899	BACHIC1D5-37A	2	-4.51	3315	70	3538	Plant fragment
128463	BACHIC1D6-25B	2	-5.27	4005	60	4479	Wood
128464	BACHIC1D7-4B	2	-5.85	4350	80	4921	Charcoal
128465	BACHIC1D7-5A	2	-5.87	4420	70	5003	Achenes
128466	BACHIC1D7-25A	2	-6.27	4450	70	5103	Achenes
128467	BACHIC1D7-47A	2	-6.71	4890	70	5625	Achenes
130293	BACHIC1D8-4B	2	-6.85	4955	70	5681	Charcoal
128468	BACHIC1D8-5A	2	-6.87	4935	70	5656	Achenes
126819	BACHIC1D8-14A	2	-7.05	5085	80	5818	Achenes
128470	BACLC3D1-7A	2	-6.45	4150	70	4694	Achenes
128435	BACLC3D1-7B	2	-6.45	4170	80	4711	Charcoal
130032	BACLC3D1-20A,21A,22A	6	-6.75	4470	70	5160	Achenes
130033	BACLC3D1-37B,38A	4	-7.07	4585	60	5308	Charcoal
128471	BACLC3D1-44B	2	-7.19	3940	140	4377	Granular fragment
130294	BACLC3D1-45C	2	-7.21	4700	70	5407	Granular fragment
128472	BACLC3D2-6B	2	-7.41	4960	60	5685	Charcoal
128476	BACLC3D2-49A	2	-8.27	5720	70	6511	Achenes
128436	BACLC3D2-49B	2	-8.27	4440	70	5046	Granular fragment
128477	BACLC3D3-5Ax	2	-8.39	5670	60	6450	Achenes

126720	BACLC3D3-5B	2	-8.39	5690	70	6470	Plant fragment
126709	BACLC3D3-7A	2	-8.43	5680	70	6460	Achenes
128478	BACPTCC1D1-2A	2	-6.84	4415	70	4994	Charcoal
128479	BACPTCC1D1-3A	2	-6.86	4495	70	5166	Achenes
130034	BACPTCC1D1-17A	2	-7.14	4700	80	5413	Achenes
130295	BACPTCC1D1-17B	2	-7.14	4645	80	5404	Charcoal
128480	BACPTCC1D1-44A	2	-7.68	5390	70	6213	Achenes
126710	BACPTCC1D2-5A	2	-7.88	5475	70	6281	Achenes
126721	BACPTCC1D2-5B	2	-7.88	5445	70	6244	Charcoal
128481	BACPTCC1D2-5C	2	-7.88	5325	70	6101	Plant fragment
130039	BRIC4D2-8A	2	0.10	235	70	277	Achenes
128482	BRIC4D2-15A	2	-0.04	165	70	174	Achenes
128437	BRIC4D2-15C	2	-0.04	350	70	398	Plant fragment
130040	BRIC4D3-7A	2	-0.37	135	80	137	Achenes
128483	BRIC4D4-3A	2	-0.53	420	70	487	Achenes
130041	BRIC4D4-26A	2	-0.99	1095	90	1006	Achenes
136900	BRIC4D525A-C,26A	4	-1.99	2075	60	2045	Seed, charcoal, insect, seed
128484	BRIC4D6-47A	2	-3.41	2970	70	3151	Achenes
128485	BRIC4D6-48A	2	-3.43	2875	70	3002	Plant fragment
128486	BRIC4D7-4A	2	-3.55	3100	70	3328	Achenes
130043	BRIC4D7-25A	2	-3.97	3225	70	3440	Achenes
128487	BRIC4D7-48A	2	-4.43	3390	60	3637	Achenes
128488	BRIC4D7-49A	2	-4.45	3485	70	3762	Achenes
128489	BRIC4D8-3A	2	-4.53	3440	70	3700	Achenes
133384	BRIC4D8-28A	2	-5.03	3535	70	3814	Charcoal
128490	BRIC4D8-41B	2	-5.29	3615	70	3925	Plant fragment
128491	BRIC4D8-41C	2	-5.29	3645	70	3962	Charcoal
128438	BRIC4D8-41D	2	-5.29	3705	70	4042	Plant fragment
126711	BRIC4D9-9A-C,10A	4	-5.67	3840	80	4254	Achenes
126722	BRIC4D9-10B	2	-5.67	3705	60	4040	Charcoal
126723	BRIC4D9-10C	2	-5.67	3765	70	4130	Plant fragment
130044	BRIC4D9-24A	2	-5.95	3700	70	4038	Achenes
130296	BRIC4D9-24C	2	-5.95	3800	70	4188	Plant fragment
130045	BRIC4D9-47A	2	-6.41	3840	70	4252	Achenes
130046	BRIC4D10-3A	2	-6.53	3890	70	4330	Achenes

130297	BRIC4D10-3C	2	-6.53	3765	60	4129	Charcoal
130298	BRIC4D10-3D	2	-6.53	3910	70	4346	Plant fragment
133137	BRIC5D8-8A	2	-5.63	3250	70	3469	Achenes
133138	BRIC5D8-8B	2	-5.63	3265	70	3492	Charcoal
133139	BRIC5D8-40A,41A	4	-6.29	4450	70	5103	Achenes
133140	BRIC5D9-25A	2	-6.97	4680	70	5400	Achenes
133385	BRIC5D9-41A	2	-7.29	4790	70	5518	Achenes
133386	BRIC5D9-41B	2	-7.29	4810	70	5520	Charcoal
133141	BRIC5D10-7A	2	-7.61	5050	70	5819	Achenes
133142	BRIC5D10-26A	2	-7.99	5240	90	5998	Achenes
133143	BRIC5D10-47A	2	-8.41	5405	60	6234	Achenes
133144	BRIC5D11-7A	2	-8.61	5410	70	6233	Achenes
128492	FWC2D1-25A	2	-0.23	140	60	142	Achenes
128493	FWC2D1-26A	2	-0.25	215	70	184	Plant fragment
130299	FWC2D3-21B	2	-2.15	1610	80	1488	Plant fragment
130049	FWC2D4-26B	2	-3.25	2530	80	2606	Charcoal
130050	FWC2D5-23A,24A	4	-4.21	3140	70	3370	Charcoal
130051	FWC2D6-26A	2	-5.25	4040	80	4513	Achenes
130052	FWC2D6-48A	2	-5.69	4435	70	5034	Achenes
128494	FWC2D6-49A	2	-5.71	4470	70	5160	Achenes
128495	FWC2D7-4A	2	-5.81	4710	70	5440	Achenes
130053	FWC2D7-26A	2	-6.25	4070	70	4561	Achenes
128496	FWC2D7-36A	2	-6.45	4160	70	4704	Achenes
130054	FWC2D7-41B	2	-6.55	4490	120	5145	Charcoal
128497	FWC2D7-43B	2	-6.59	4510	70	5163	Charcoal
126712	FWC2D8-5B	2	-6.83	4340	80	4914	Achenes
128439	FWC2D8-5E	2	-6.83	4195	60	4733	Plant fragment
128440	FWC2D8-5F	2	-6.83	4145	70	4689	Plant fragment
130055	SHERCIC3D1-2A	2	-5.48	4005	70	4479	Achenes
130056	SHERCIC3D1-12A	2	-5.68	4225	70	4751	Achenes
130057	SHERCIC3D2-6A	2	-5.78	4110	70	4636	Achenes
130058	SHERCIC3D2-23A	2	-6.12	4560	70	5173	Achenes
130059	SHERCIC3D3-2A	2	-6.19	4590	70	5311	Achenes
130060	SHERCIC3D3-24A	2	-6.63	5010	90	5749	Achenes
130300	SHERCIC3D3-25A	2	-6.65	5060	70	5819	Charcoal
130097	SHERCIC3D4-8A	2	-6.81	5115	80	5827	Achenes
126713	SHERCIC3D4-15A	2	-6.95	5425	80	6237	Achenes

130098	SHERLC2D1-13A	2	-4.95	3400	80	3649	Achenes
130099	SHERLC2D2-4A	2	-5.05	3520	120	3794	Achenes
130100	SHERLC2D2-34A	2	-5.65	4160	140	4689	Charcoal
130101	SHERLC2D3-10B	2	-5.87	3980	120	4450	Charcoal
130102	SHERLC2D3-28A	2	-6.23	4010	200	4497	Charcoal
130400	SHERLC2D3-28B	2	-6.23	4280	80	4850	Granular fragment
130103	SHERLC2D4-24A	2	-7.15	4950	120	5687	Charcoal
130104	SHERLC2D4-46A	2	-7.59	5530	70	6331	Achenes
126714	SHERLC2D4-47A	2	-7.61	5670	70	6451	Achenes
126724	SHERLC2D4-47B	2	-7.61	5740	140	6540	Charcoal
130105	TTC3D1-22A	2	-0.24	60	70	97	Achenes
130106	TTC3D2-45A	2	-1.68	1265	70	1214	Achenes
126715	TTC3D5-13A	2	-4.04	2315	70	2338	Achenes
130107	VICIC2D1-2A	2	-7.44	3980	70	4467	Achenes
130108	VICIC2D2-8A	2	-7.71	4430	70	5021	Achenes
130401	VICIC2D2-8B	2	-7.71	4430	80	5027	Charcoal
130402	VICIC2D4-8B	2	-8.31	5400	120	6202	Granular fragment
130109	VICIC2D4-9A	2	-8.33	5530	70	6331	Achenes
130110	VICIC2D4-19A	2	-8.53	5620	70	6397	Achenes
130403	VICIC2D4-19B	2	-8.53	5740	70	6538	Plant fragment
136901	VIPPC4D3-18A	2	-6.24	4070	120	4580	Plant fragment
130404	VICIC2D4-38B	2	-8.91	5800	160	6600	Charcoal
126716	VICIC2D4-39A	2	-8.93	5870	70	6694	Achenes
130111	VIPPC4D1-8A	2	-5.04	3085	70	3307	Charcoal
130112	VIPPC4D4-25A	2	-7.36	4990	70	5714	Achenes
130113	VIPPC4D4-49A	2	-7.84	5300	70	6083	Achenes
130114	VIPPC4D5-5A	2	-7.96	5410	90	6225	Achenes
126717	VIPPC4D5-22A	2	-8.30	5790	70	6591	Achenes
126725	VIPPC4D5-23B	2	-8.32	5610	200	6406	Charcoal
126726	VIPPC4D5-23C	2	-8.32	5730	100	6528	Plant fragment
130115	WTCIC2D1-3A	2	-7.92	4090	80	4604	Achenes
130116	WTCIC2D1-7A	2	-7.99	4355	80	4925	Achenes
130117	WTCIC2D2-4A	2	-8.08	4715	70	5453	Achenes
130118	WTCIC2D2-12A	2	-8.24	4825	70	5530	Achenes
130388	WTCIC2D3-4B	2	-8.33	5075	80	5817	Charcoal
130389	WTCIC2D3-21A	2	-8.67	5105	70	5818	Achenes
130405	WTCIC2D3-21C	2	-8.67	5330	70	6107	Charcoal
130390	WTCIC2D4-4A	2	-8.77	5655	90	6437	Achenes
130406	WTCIC2D4-4B	2	-8.77	5385	80	6203	Charcoal

130391	WTCIC2D4-12A	2	-8.93	5670	70	6451	Achenes
130392	WTCIC2D5-2C	2	-9.07	5820	60	6634	Achenes
126718	WTCIC2D5-3A	2	-9.09	5800	70	6601	Achenes
126727	WTCIC2D5-3B	2	-9.09	5920	560	6769	Charcoal
130393	WTLC3D1-10A	2	-6.72	3825	70	4223	Charcoal
130394	WTLC3D2-5A	2	-7.09	4300	60	4858	Charcoal
130395	WTLC3D3-8A	2	-7.63	4750	70	5513	Plant fragment
130396	WTLC3D4-21B	2	-8.20	5500	80	6300	Granular fragment
130397	WTLC3D4-35A	2	-8.48	5765	70	6567	Achenes
126719	WTLC3D5-8A	2	-8.68	5830	80	6643	Achenes
126728	WTLC3D5-8B	2	-8.68	5905	60	6722	Charcoal
Shlemon and Begg (1975)	Devils Is., 0.9m	unknown	0.9*	860	170	809	Bulk peat
Shlemon and Begg (1975)	Devils Is., 2.4m	unknown	2.40*	2420	140	2495	Bulk peat
Shlemon and Begg (1975)	Devils Is., 4.0m	unknown	4.00*	3575	260	3905	Bulk peat
Shlemon and Begg (1975)	Terminus Is. 6.1m	unknown	6.10*	3315	150	3564	Bulk peat
Shlemon and Begg (1975)	W. Sherman Is. 6.1m	unknown	6.10*	3900	140	4327	Bulk peat
Shlemon and Begg (1975)	Twitchell Is., 6.1m	unknown	6.10*	3090	190	3276	Bulk peat
Shlemon and Begg (1975)	Sherman Is., 9.1m	unknown	9.10*	4340	195	4948	Bulk peat
Shlemon and Begg (1975)	Andrus Is., 9.1m	unknown	9.10*	4675	200	5359	Bulk peat
Shlemon and Begg (1975)	Sherman Is., 12.2m	unknown	12.20*	6635	320	7501	Bulk peat
Shlemon and Begg (1975)	Sherman Is. 15.2m	unknown	15.20*	6805	350	7668	Bulk peat
Atwater et al.	borehole 35	unknown	-7.90	3360	105	3608	Salt marsh

(1977)							plant roots
Atwater et al. (1977)	borehole 25	unknown	-6.60	3930	105	4365	Salt marsh plant fragments
Atwater et al. (1977)	borehole 36	unknown	-9.00	5745	185	6562	Salt marsh plant roots
Atwater et al. (1977)	borehole 32	unknown	-11.40	5845	100	6656	Forams and/or diatoms
Atwater et al. (1977)	borehole 33	unknown	-10.80	6200	320	7053	Forams and/or diatoms
Atwater et al. (1977)	borehole 21	unknown	-9.20	6855	115	7708	Unknown
Atwater et al. (1977)	borehole 11	unknown	-24.60	8230	135	9201	Forams and/or diatoms
Atwater et al. (1977)	borehole 10	unknown	-21.00	8295	135	9270	Forams and/or diatoms
Atwater et al. (1977)	borehole 16	unknown	-18.70	8365	135	9337	Forams and/or diatoms
Shlemon and Begg (1975)	Devils Is., 9m	unknown	0.9*	860	170	809	Bulk peat
Shlemon and Begg (1975)	Devils Is.,2.4m	unknown	2.40*	2420	140	2495	Bulk peat
Shlemon and Begg (1975)	Devils Is., 4.0m	unknown	4.00*	3575	260	3905	Bulk peat
Shlemon and Begg (1975)	Terminus Is., 6.1m	unknown	6.10*	3315	150	3564	Bulk peat
Shlemon and Begg (1975)	W. Sherman Is., 6.1m	unknown	6.10*	3900	140	4327	Bulk peat
Shlemon and Begg (1975)	Twitchell Is., 6.1m	unknown	6.10*	3090	190	3276	Bulk peat
Shlemon and Begg (1975)	Sherman Is., 9.1m	unknown	9.10*	4340	195	4948	Bulk peat

Shlemon and Begg (1975)	Andrus Is., 9.1m	unknown	9.10*	4675	200	5359	Bulk peat
Shlemon and Begg (1975)	Sherman Is., 12.2m	unknown	12.20*	6635	320	7501	Bulk peat
Shlemon and Begg (1975)	Sherman Is., 15.2m	unknown	15.20*	6805	350	7668	Bulk peat